Published in final edited form as:
Math Biosci. 2010 August ; 226(2): 77–96. doi:10.1016/j.mbs.2010.05.001.

Pulse Coupled Oscillators and the Phase Resetting Curve

Carmen C. Canavier[1,2] and **Srisairam Achuthan**[1]

[1]Neuroscience Center of Excellence, New Orleans, LA 70112

[2]Dept. of Ophthalmology, LSU Health Sciences Center, New Orleans, LA 70112

Abstract

Limit cycle oscillators that are coupled in a pulsatile manner are referred to as pulse coupled oscillators. In these oscillators, the interactions take the form of brief pulses such that the effect of one input dies out before the next is received. A phase resetting curve (PRC) keeps track of how much an input advances or delays the next spike in an oscillatory neuron depending upon where in the cycle the input is applied. PRCs can be used to predict phase locking in networks of pulse coupled oscillators. In some studies of pulse coupled oscillators, a specific form is assumed for the interactions between oscillators, but a more general approach is to formulate the problem assuming a PRC that is generated using a perturbation that approximates the input received in the real biological network. In general, this approach requires that circuit architecture and a specific firing pattern be assumed. This allows the construction of discrete maps from one event to the next. The fixed points of these maps correspond to periodic firing modes and are easier to locate and analyze for stability compared to locating and analyzing periodic modes in the original network directly. Alternatively, maps based on the PRC have been constructed that do not presuppose a firing order. Specific circuits that have been analyzed under the assumption of pulsatile coupling include one to one lockings in a periodically forced oscillator or an oscillator forced at a fixed delay after a threshold event, two bidirectionally coupled oscillators with and without delays, a unidirectional N-ring of oscillators, and N all-to-all networks.

Keywords

Pulse coupled oscillators; Phase resetting; Phase locking; Synchronization; Splay; Clustering

INTRODUCTION

I.1 Scope

The study of synchronization and phase locking in networks of coupled oscillators was pioneered by Kuramoto ([1]), Winfree ([2]), Glass and Mackey ([39]) and Pavlidis ([68]). In this article, we review the literature on pulse coupled oscillators. In contrast to diffusive coupling which is always active, the duration of the interactions between pulse coupled oscillators is so brief compared to the network period as to render the coupling effectively pulsatile. The coupling between neurons that communicate via chemical synapses is an

Corresponding Author: Srisairam Achuthan, Neuroscience Center, 2020 Gravier St., Suite D, New Orleans LA 70112, sachut@lsuhsc.edu, 504-599-0915 phone, 504-568-5801 fax.

example of pulsatile coupling, as is the coupling between fireflies that emit brief regular light flashes, for example. The usual approach to studying pulse coupled oscillators is to construct a map by strobing the system ([3]) that is, sampling it just before and just after each pulse. A return map can be constructed from the phases just after a pulse to the phases just after the next pulse. We first describe a very general nonlinear map that is difficult to analyze, and use this map to show that in principle, any firing pattern exhibited by a pulse coupled network can be exhibited by the map using only the phase resetting curve (PRC). We then describe a different class of maps, in which a particular firing pattern is assumed, which allows the linearization of the map about the presumed fixed point and the determination of the stability of this fixed point, if it indeed exists. We presume a neural context and refer to the oscillators as neurons, but the analysis is general and applies to any type of pulse coupled oscillator.

I. 2 Definition of the PRC for pulse coupling

There are two general approaches that we review here. One mathematical approach is to assume a form for the oscillator and for the nature of the pulsatile coupling in such a way that implicitly defines a PRC ([3]–[6]). Another, more biological, approach is to leave the form of the PRC unspecified, but to assume that it describes the response of an oscillator to the input that it will receive in the network. In section IV.5 we conclude that the latter approach includes the former as a special case.

For applications with pulsatile coupling, the relevant PRC is either estimated or generated (see Fig. 1) directly with the input stimulus waveform that each neuron in the network receives ([7]–[11]). The PRC can be measured in an open loop configuration (see Fig. 1A) such that it receives input from the neuron(s) that will be pre-synaptic to it in the closed loop network configuration, but is isolated in that it does not affect the driving pre-synaptic neuron. The advantage of this approach is that it can be applied to real oscillators for which the governing differential equations are unknown. In the example shown (the PRC protocol in Fig.1B), this input is the synaptic conductance waveform (lower trace Fig. 1B) that results from an action potential in the pre-synaptic neuron, such that the PRC is equivalent to the spike time response curve - STRC ([12], [13]). Although spiking neurons are used in this illustration, the same procedure applies to bursting neurons except that burst onset rather than spike onset is assigned a phase of zero, and the perturbation in conductance results from a pre-synaptic burst rather than a single action potential. In the open loop condition (i.e. when there is only a single unidirectional coupling) the phase at which a stimulus is received is $\phi = ts/T_0$, where T_0 is the intrinsic period and ts is the time between the last action potential in the model neuron for which the PRC is being generated and the action potential initiation in the pre-synatic model neuron. The normalized change in the length of the cycle containing the perturbation and the one following it are called the first order phase resetting, $f_1(\phi)=(T_1 - T_0)/T_0$, and second order phase resetting, $f_2(\phi)=(T_2 - T_0)/T_0$, respectively. T_1 is the length of the cycle containing the perturbation and T_2 is the length of the subsequent cycle (see Fig. 1C). Plotting the resetting with this convention, often used by biologists, causes a delay to be positive and an advance negative, in contrast to the opposite convention often used by mathematicians. The permanent resetting, meaning the phase shift that remains after all transients due to the perturbation have dissipated is the sum of the resetting on all cycles subsequent to the perturbation, has been used in some contexts ([2], [39], [66]), but here we treat the effect on each cycle following the perturbation separately. Fig. 1D shows the PRCs for two conductance values, one of which is twice the first. Clearly, doubling the strength of the perturbation does not double the resetting observed at all phases, so the dependence of the resetting on the strength of perturbation is nonlinear, in contrast to the linearity assumed by the weak coupling approach described in section IV.5.

I.3 Motivation

Much previous work on applications of PRC was dominated by a need to study entrainment by an external periodic stimulus ([2], [39]), motivated by applications such as the pacing of abnormal cardiac rhythms by applying appropriate perturbations, neural stimulation of respiratory oscillators, and the entrainment of circadian oscillators (clocks) by light stimuli. Here we address periodic forcing in III.1.1, but the remainder of the article deals with the self-organization of networks of oscillatory neurons. The problem of studying pulse coupled oscillators in a neural context can be subdivided into two parts. Here, we will address one part; how the PRCs of the component neurons in a network determine what patterns of network activity will be produced. The second part of the problem is how the individual ionic and synaptic currents lead to a particular PRC ([73], [74], [76] and [84]) and is not addressed here. However, combining these two parts would eventually allow for a thorough understanding of how pharmacological targeting of biophysical parameters such as conductances in particular neurons would affect the overall network activity.

To date, the neural applications of the PRC based theory of pulse coupled oscillators are not yet mature in that they have not yet been widely applied to obtain useful insights into cognition, motor behavior or disease. The potential is huge however. Phase resetting theory has been applied to attempt to desynchronize the pacemakers underlying Parkinsonian tremor ([77]). Phase resetting theory has also been applied to the study of desynchronization in a model of epilepsy ([78]). Furthermore, it is likely that phase resetting can be applied to understand the physiology of cognition and movement. Phase resetting of 7–16 Hz oscillations in human neocortex ([79]) has been proposed to underlie human working memory. Phase resetting in the inferior olive nucleus has been proposed as a mechanism for motor error correction ([80]). Phase resetting theory can be applied to understanding spinal pattern generators for rhythm and locomotion, and for the synchronization that gives rise to measurable EEG signals in many frequency bands such as theta, alpha, beta, and gamma ([37]). The impact of the theory of pulse coupled oscillators on neuroscience has yet to manifest itself fully, but there is certainly the potential for both great advances in the understanding of cognitive function and for therapeutic breakthroughs of clinical relevance.

II Map with no predetermined firing order (NPFO)

II.1 How is the nonlinear iterative map defined ?

The key feature of this type of map is that it has no predetermined firing order. The NPFO map can be conceptualized ([8]) as a modified Winfree ([2]) model,

$$d\phi_j/dt=\omega_j - f_{1jk[mj]}(\phi_j[m_j])\,\delta\,(t[m_j]) - f_{2jk[mj]}(\phi_j[m_j-1])\,\delta\,([\phi_j=0]) \quad (1)$$

where m_j is the m^{th} input received by neuron j, ϕ_j is the phase of the j^{th} neuron and f_{gjk} is the g^{th} order resetting produced in neuron j by any subset $k[m_j]$ of simultaneously arriving pulses from other spiking neurons. In between pulses, the phase of each neuron increases at a rate determined by its intrinsic frequency ω_j. When a phase of one is reached a pulse is emitted and the phase is reset to zero. The first order resetting is applied at the time $t[m_j]$ the pulse is received by neuron j. The time that the pulse arrives in a system with no delay is the time when the subset k spikes, that is when the phase reaches one (ϕ =1) for each neuron in the spiking subset. A conduction delay may be added to the spike time to determine the arrival time of each pulse. For a rigorous implementation of pulsatile coupling, the effect of one input is assumed to die out before the next one is received, therefore the second order resetting due to any input is assumed to be negligible if another input is received before the receiving neuron fires again (but see section II.3). When neuron j fires and ϕ_j is reset to zero, the second order resetting from the most recent input is added.

The implementation of this conceptual map is highly nonlinear. One nonlinear step involves polling the neurons to determine which neuron or neurons will fire next since no a priori assumptions are made about the order in which neurons will fire, or if they will fire at all. The other nonlinearity is that the rules by which the phases are updated at each event depend upon the neuron that fires (emits a pulse) during an event, and on whether it receives an input during the event. Here we index the n^{th} pulse emission in the system, and we also index the arrival of the pulse as m_j depending upon which neuron received the pulse. The same event may be received by multiple neurons, so the indexing scheme is as uncontrained as the firing order. For simplicity we will describe a map with no delays here.

The connectivity matrix for a network of N neurons is an N by N matrix W in which the element w[i,j] is 1 if the i^{th} neuron sends a pulse to the j^{th} oscillator and 0 otherwise. A g^{th} order PRC f_{gjk} must be known in the j^{th} oscillator for the combined pulses from every possible subset C_{jk} of the set of oscillators C_j for which w[i,j] = 1 since we do not assume that the phase resetting due to the pulses sums linearly. Thus the map becomes very complex unless we assume either identical oscillators or a small number of oscillators or sparse connectivity.

To start the map iterations, we arbitrarily initialize all phases $\phi_j[0]$ and the saved second order resetting $f_{2jk}(\phi_j[0])$ for each oscillator at event zero (not necessarily a spiking event, although all subsequent events in this version are with no conduction delays). $\phi_j[n]$ is the phase of oscillator j after all the effects of the previous pulse were added, where n refers to the n^{th} cycle number. The map equations below then determine which neuron (s) will spike next based on how long it will take for the current phase to reach one given the intrinsic period of each neuron (P_j). All oscillators that emit a pulse at event n are members of S[n] and all oscillators that receive a pulse from at least one of the members of S[n] are a member of set R[n]. The set $C_{jk}[n]$ of neurons in S[n] that send pulses to neuron j in R[n] at each spiking event n allows us to index jk[n] for each event and for each oscillator in order to access the correct PRCs.

$$\text{If } P_j(1-\phi_j[n]) = \min_{u\in\{1,\ldots,N\}}\{P_u(1-\phi_u[n])\} \text{ then } j\in S[n] \text{ else } j\notin S[n]$$

$$\text{If } \sum_{i\in S[n]} w[i,j] \geq 1 \text{ then } j\in R[n] \text{ else } j\notin R[n]$$

$$\text{for } i\in S[n] \text{ and } j\in R[n] \text{ if } w[i,j]=1, \text{ then } i\in C_{jk}[n] \text{ else } i\notin C_{jk}[n]$$

$$\begin{aligned}
\phi_j[n+1] &= 0 - f_{2jk[mj-1]}(\phi_j[m_j-1]) && \text{if } j\in S[n], j\notin R[n]\\
&= 0 - f_{2jk[mj-1]}(\phi_j[m_j-1]) - f_{1jk[n]}(\phi_j[n]+(t[n+1]-t[n])/P_j) && \text{if } j\in S[n], j\in R[n]\\
&= \phi_j[n]+(t[n+1]-t[n])/P_j - f_{1jk[n]}(\phi_j[n]+(t[n+1]-t[n])/P_j) && \text{if } j\notin S[n], j\in R[n]\\
&= \phi_j[n]+(t[n+1]-t[n])/P_j && \text{if } j\notin S[n], j\notin R[n]
\end{aligned}$$

where $t[n+1]-t[n] = \min\{P_j(1-\phi_j[n])\}$ over all j where P_j is the intrinsic period of neuron j.

Note that m_j refers to the same event as n, but m_j-1 does not necessarily refer to the same event as n−1. The second order resetting terms are only nonzero if they do refer to the same event. There are four ways in which the phase can be updated. All phases are advanced from just after pulse n to just before pulse n by $(t[n+1] - t[n])/ P_j$ and if an oscillator neither emits nor receives a pulse at this event, it is only updated by this amount. In the case that the oscillator emits a pulse in this event, the advancement of the phase causes the phase to reach 1 and be reset to zero, then the stored second order resetting from the last event in the previous cycle is subtracted. In the case that the oscillator receives a pulse in this event, then the first order resetting from the last event in the previous cycle is subtracted after the phase is advanced. Finally, if an oscillator both emits and receives a pulse, then both first and second order resetting will be subtracted.

If delays are considered, pulse emission and the receipt of a pulse occur at different times, such that there are two classes of events. The difference is in how the time to the next event is computed; it must now be computed regardless of whether the next event is the emission of a pulse or the receipt of a pulse. All phases must be updated to the next event, and then the first order resetting is added to the phase for pulse receipt events and the second order for pulse emission events. In this case, $t[n+1] - t[n] = \min \{P_j (1 - \phi_j[n]), e[q,i] + \tau[i,j] - t[n]\}$ over all j and q. Here, n refers to either pulse emission or receipt, e[q,i] refers to pulse emission for pulses indexed by q from each neuron i that has not reached all neurons j for which w[i,j] = 1, that is $e[q,i] + \tau[i,j] > t[n]$, where $\tau[i,j]$ is the conduction delay from a pulse emitted by neuron i until its receipt at neuron j.

Set membership is now defined as

$$\text{If } t[n+1]=P_j (1-\phi_j[n])=\min_{u\in\{1,\ldots,N\}}\{P_u (1-\phi_u[n])\} \quad \text{then } j \in S[n] \text{ else } j \notin S[n]$$

$$\text{If } t[n+1]=e[q,i]+\tau[i,j]-t[n] \text{ and } \sum w[i,j]=1 \text{ then } j \in R[n] \text{ else } j \notin R[n]$$

$$\text{If } e[q,i]+\tau[i,j]-t[n]=\min\{P_j (1-\phi_j[n]), e[q,i]+\tau[i,j]-t[n]\}, j \in R[n] \text{ and } w[i,j]=1,$$

$$\text{then } i \in C_{jk}[n] \text{ else } i \notin C_{jk}[n].$$

Otherwise the map is the same. The problem with analyzing either map is that, on each iteration, the rules for updating the phase of each oscillator can change between four possible variants. This same complexity endows the map with the ability to capture the full richness of the oscillatory solutions that a noiseless pulse coupled system can exhibit, under the conditions that full information regarding network connectivity and phase resetting is available and that all assumptions underlying the map are met. The map is a reduction of the full dynamics of a system to an ideal pulse coupled system. Both model neurons and real neurons can be reduced to the map using the PRC as described in I.2, under the conditions described above. The full systems are only approximately pulsatile; therefore discrepancies between the output of the map and that of the full system are usually caused by a failure of the strict pulsatile coupling assumption in the full system, as described below (see II.3).

II.2 Computational results for networks of two and four neurons using the NPFO map

Figure 2 illustrates how the map described in the previous section is able to reproduce very complex patterns of activity using only the phase resetting curves and the intrinsic periods of the component neurons. Networks of Wang and Buzsaki model neurons ([14]) coupled with reciprocal inhibition between all neurons were used to test the map above. No conduction delays were considered, and the connectivity matrix is one everywhere except on the diagonal where i=j because autapses were not considered. Figure 2A and 2B were adapted from Figs. 8 C and 8D of ([15]) and illustrates the case for two neurons as the difference in intrinsic frequency between the two neurons is increased by applying different levels of bias current (ε on the x-axis) to each model neuron. In a two neuron system, each neuron only receives input from one other neuron, so the receipt of multiple simultaneous inputs is not possible, which greatly simplifies the map. For clarity, only a subset of the intervals t[n+1] – t[n] are plotted such that the $(n+1)^{st}$ event was a spike in a one specific oscillator and not in the partner neuron. The transients after initializing the map were allowed to die out. A steady mode was achieved if increasing the number of events did not increase the distinct values of t[n+1] – t[n] that were obtained and plotted in Fig. 2A, where Fig. 2A1 shows the output of the NPFO map and Fig. 2A2 shows the output obtained by integrating the full system of differential equations. In patterns in which the firing order remained constant in a 1:1 periodic locking, only a single dot is observed for near synchronous lockings in which the same neuron always fired first and t[n+1] – t[n] had a small value (blue dots). For low values of the heterogeneity parameter (nearly identical frequencies), the firing order was able to switch every other cycle ([15], [16]), so the large intervals (green dots) correspond to two successive firings in the reference neuron, followed by two successive firings in the partner neuron. Note the ability of the map to accurately reproduce very complex patterns (black dots). In addition, an antiphase firing mode was bi-stable with the modes shown for $\varepsilon < 0.06\ \mu A/cm^2$ (not shown). Depending upon the initial conditions, in this parameter range the NPFO map could reproduce the modes shown as well as the antiphase mode, capturing the bistability of the full system.

Figs. 2C and 2D show that the above approach can easily be extended to higher size networks. Figures 2C and 2D were adapted from Fig. 7 of ([17]) and illustrate the case for four Wang and Buzsaki model neurons ([14]) with reciprocal inhibition as the synaptic conductance strength between the neurons is increased. Some common observed modes are the fully synchronous mode (one cluster of four neurons), the splay firing mode (four clusters of 1 each) and the two clusters of two neurons in antiphase ([17]). All of these are represented by a single firing interval where simultaneous firings are counted as a single event. Bistability is seen at weak conductance strengths between the fully synchronous mode and two clusters of two neurons in the antiphase mode. Other complex modes that are observed are shown as well ([17]). Synchronous modes in which the firing times of all four neurons are not exact are represented by the closed blue diamonds. The closed red circles represent two clusters of two neurons where the short intervals indicate that near synchronous mode within each cluster. Finally, the closed green squares represent a near splay mode in which the four intervals are not exactly equal to each other. The yellow stars represent intervals from complex periodic modes with a period of many cycles, or in some cases aperiodic modes. Both the periodic as well as aperiodic observed modes were accurately captured by the NPFO map except for some small discrepancies.

II.3 Strengths and weaknesses of the NPFO approach

The strength of the map method described above is that it is an idealized pulse coupled system that can reproduce arbitrary firing patterns given only the PRCs and periods under the conditions that there is no noise, full information regarding network connectivity and phase resetting is available, and that all assumptions underlying the map are met. It is very

useful for determining whether the PRC contains sufficient information to account for network activity [19]. Maps similar to the NPFO map have been used in the past to study network dynamics ([7], [8], [13], [15]–[19]). The NPFO map easily handles multistability and aperiodic modes ([15], [17]). However, the fixed points of this map cannot easily be determined a priori due to the nonlinear step of polling for neuron(s) that will fire next. Therefore, stability criteria based on the slopes of the PRC cannot be derived from this map, which limits the intuitive understanding of synchronization and phase locking that can be derived from this method. For this reason, PFO maps with a predetermined firing order are derived in the next section.

One important issue with respect to the NPFO map is that causality can never be violated. In practice, this implies that the recovery interval between when an input is received and when the next spike is generated must be nonnegative. This is important when noise is added to the map. Specifically, the first order resetting cannot advance the next spike to a time point before the input is received; when random noise is added such advances could occur by chance, but must be discarded as impossible. The stimulus interval between when a neuron fires and when it receives its next input must also be nonnegative. Therefore the second order resetting that is applied after a given spike can advance the phase until the phase at which the next input is received, but no farther.

There are some subtle problems with simultaneous input at synchronization. For example, it is possible to receive an input when the phase resetting is undefined, specifically during the period that the phase is negative. A negative phase can occur immediately after spiking when the second order resetting is a delay. Since a negative phase does not actually correspond to a point on the limit cycle in this case ([16]), the resetting assigned to the second pulse is arbitrary. In the NPFO maps shown in Fig. 2, at negative phases the nearest value for resetting, i.e., the resetting at a phase of zero, was assigned to all negative phases. Thus, this can introduce error near synchrony.

The assumption of pulsatile coupling dictates that when two inputs are received in succession, all of the resetting due to the first input is assumed to be complete by the time the second input is received. If the two inputs arrive close together during synchronization, this assumption may not be valid. For example, the presumed resetting due to two identical pulses separated by a normalized delay τ is $f(\phi) + f(\phi - f(\phi) + \phi)$ ([19]). A discontinuity in the NPFO map can occur near synchrony as follows. In the limit as τ approaches zero, the resetting due to two sequential pulses calculated as described under the pulsatile coupling assumption does not necessarily approach the observed resetting due to the combined pulse because of potential nonlinear interactions between the pulses. These interactions are not measured during the PRC protocol, which uses a single pulse, and may cause a violation of the assumption of pulsatile coupling as the separation between pulses becomes smaller.

Another weakness of the NPFO map is that there is a conflict between the strict memoryless assumption and the symmetry requirement of exact synchrony. The assumption of pulsatile coupling requires a memoryless system in which the resetting due to one input is complete by the time the next input is received means that the system is memoryless. This assumption dictates that second order resetting due to inputs that do not immediately precede an action potential be ignored. However, in a system with more than two neurons, a memoryless NPFO map can fail to reproduce the fully synchronous mode or synchronous sub-clusters in some cases ([17]); ignoring the second order resetting except that due to the last input received in a cycle very slightly disrupts the symmetry required to achieve exact synchrony. If all second order resetting is taken into account, the memoryless assumption is somewhat relaxed, but symmetry is preserved allowing global synchrony to be achieved in the problematic cases identified above. However, including all second order resetting can

disrupt ability of the pulse coupled map to reproduce the splay mode in some cases ([17]) due to a causality violation as described above. The exact implementation of the map with respect to second order resetting that is appropriate varies depending upon the system. Although mismatches between the performance of the full system and the NPFO have been identified for a small subset of parameter sets that have been examined, in general very good agreement is observed in a wide variety of cases over large parameter regimes.

One distinction between the PRC for a model neuron and that for a biological neuron is that the PRC for the biological neuron is unavoidably noisy. Noise can be incorporated in the map by randomizing the phase resetting. The use of statistical methods to determine whether there is a locking ([51]) becomes necessary in the presence of noise. There are examples in the literature of both noiseless ([8], [15]–[17]) and noisy ([18], [33], [54]) NPFO maps.

III. Maps with predetermined firing order (PFO maps)

Another approach involves the construction of a map in which a specific firing pattern is always assumed. In such a case, the oscillators fire with a predetermined firing order (PFO). The most general forms of these maps do not assume anything about the equations for the endogenous oscillators or the synaptic dynamics. We designate these results as applicable to arbitrary PRCs. Other approaches make assumptions about the form of dynamics of the oscillator and the form of the phase resetting, implicitly defining a PRC ([53], [55]). We show that the results for implicitly defined PRCs are a subset of the more general results for arbitrary PRC.

The fixed points of the PFO maps in terms of the locked phases can be computed from a unique set of periodicity criteria that emerge from the map. The intervals between neural firings can be expressed in terms of the phase resetting under the assumption of pulsatile coupling. Then a discrete map of the intervals can be constructed. The phases that allow the appropriate intervals to remain constant constitute a fixed point of the map. Assuming a perturbation from the fixed point and linearizing the PRCs about the presumed fixed point allows the map to be rewritten in terms of the perturbations in the phases. Stability is guaranteed only when the perturbations decay to zero.

In all of the following stability proofs: Curly braces {} group terms with a common multiplier, parentheses () indicate a function, and straight brackets [] enclose the cycle number in a discrete map.

III.1 Results for a single driven neuron using the PFO map

III.1.1 Periodically forced neuron—Perkel et al. ([20]) measured the first order PRC, $f_1(\phi)$, by inducing precisely timed inhibitory or excitatory synaptic potentials in invertebrate pacemaker neurons by evoking an action potential in an excitatory or inhibitory pre-synaptic neuron. The PRC was then used to predict stable m:1 entrainment of the pacemaker neuron (the forced oscillator) by a periodic train (the forcing oscillator) of evoked synaptic potentials.

Ignoring second order resetting, the length of a cycle that includes a perturbation is $P_f = P_0\{1 + f_1(\phi)\}$ (see Fig. 3), where P_f is the period of the forcing neuron, P_0 is the intrinsic period of the forced neuron and $f_1(\phi)$ is the first order phase resetting. For m:1 phase lockings in which only every m^{th} cycle contains a perturbation:

$$P_f=\{m-1\}P_0+P_0\{1+f_1(\phi^*)\} \quad (2)$$

where ϕ^* is the steady phase at which an input is received in a phase locked mode. Thus, all possible m:1 lockings can be determined from the PRC alone by finding which phases, if any, satisfy the equality. Stable phase lockings were determined by Perkel et al. using an analytically derived map based on the PRC of the forced oscillator. The elapsed time between an action potential in the pacemaker and the arrival of a pre-synaptic potential due to the periodic forcing in the n^{th} cycle is denoted as the stimulus interval, ts[n]. Ignoring any second order resetting the stimulus interval is:

$$ts[n]=P_0\{\phi[n]\} \tag{3}$$

where ϕ[n]) is the phase of the pacemaker at the time of the receipt of an input in the n^{th} cycle. The first order resetting of the pacemaker is assumed to occur during the recovery interval, tr[n], i.e. between the receipt of an input by the pacemaker and its next spike. For 1:1 forcing, the analytically derived map is generated as follows (see Fig. 3):

$$P_0\{1+f_1(\phi[n])\}+ts[n+1]=ts[n]+P_f. \tag{4}$$

Rewriting the above equation and using the definition of P_f, we have:

$$\begin{aligned} ts[n+1]-ts[n] &= P_f - P_0\{1+f_1(\phi[n])\} \\ &= P_0\{1+f_1(\phi^*)\} - P_0\{1+f_1(\phi[n])\} \\ &= P_0\{f_1(\phi^*) - f_1(\phi[n])\} \end{aligned} \tag{5}$$

Linearizing the PRC in the neighborhood of the presumed fixed pointϕ^* produces $f_1(\phi[n]) = f_1(\phi^*) + f_i'(\phi^*)\,\Delta\phi[n]$, where the perturbation from the fixed point is given by $\Delta\phi[n] = \phi[n] - \phi^*$. The slope of the i^{th} order PRC at the locking point ϕ^* is $f_i'(\phi^*)$. The stimulus interval can be rewritten as:

$$ts[n]=P_0\{\phi[n]\}=P_0\{\phi^*+\Delta\phi[n]\}. \tag{6}$$

Substituting the stimulus interval from (6) in (5), linearizing the PRC about ϕ*and simplifying we obtain:

$$\Delta\phi[n+1]=\{1-f_1'(\phi^*)\}\,\Delta\phi[n]. \tag{7}$$

If $-1 < |1-f_1'(\phi^*)| < 1$, then $\Delta\phi$ [n+1] goes to zero and the locking at ϕ* is stable.

The stability results incorporating second order resetting were derived in ([21]). The result given above is not novel but has been rederived here in terms of the PRC convention used throughout this review.

III. 1.2 Neuron repeatedly stimulated with feedback at a fixed delay—A periodically spiking neuron forced with a feedback input at a fixed delay after each spike was shown to exhibit multi-stable phase locked modes by Foss and Milton ([22]). The original stability proof given by Foss et al. ([22]) did not assume any second order resetting. This proof is rederived below using terminology consistent with the other proofs given herein. A proof incorporating second order resetting has been presented by Canavier and Achuthan ([21]).

Fig.4 represents a periodically forced neuron with a fixed delay (δ) between any two consecutive forced inputs. The interval between the last spike and the receipt of an input in cycle n is the stimulus interval ts[n] = $P_0\{\phi[n]\}$. The interval between the receipt of an input in cycle n and the next spike is the recovery interval tr[n] = $P_0\{1-\phi[n] + f_1(\phi[n])\}$. The network period of an oscillator is the sum of its stimulus and recovery intervals. The integer k denotes the number of network periods wholly contained in the delay, δ. Using the definition of the network period of an oscillator produces the following self consistent periodicity criterion:

$$\delta = \sum_{j=n}^{n+k-1} \{ts[j]+tr[j]\}+ts[n+k]. \tag{8}$$

Using the definition of the stimulus and recovery intervals the above equation can be rewritten as:

$$\delta = P_0 \sum_{j=0}^{k-1} \{1+f_1(\phi[n+j])\}+P_0\{\phi[n+k]\} \tag{9}$$

At a steady 1:1 locked mode, all values of $\phi[n+j]$ are equal. We can find the fixed points that satisfy the equality $\delta/P_0 = k\{1 + f_1(\phi^*)\} + \phi^*$. A stability criterion can be derived by again assuming a perturbation from the fixed point such that $\phi[j] = \phi^* + \Delta\phi[j]$, and linearizing the PRCs such that $f_1(\phi[j]) = f_1(\phi^*) + f_1'(\phi^*)\Delta\phi[j]$, where $f_1'(\phi^*)$ indicates the slope of the first order PRC at the locking point, ϕ^*. If these substitutions are made in (9) above, the steady state terms are canceled from both sides, and the term for $\Delta\phi[n+k]$ is moved to the left hand side, the following linear system is obtained:

$$\Delta\phi[n+k] = -\sum_{j=0}^{k-1} \{f_1'(\phi[n+j])\}\Delta\phi[n+j] \tag{10}$$

The matrix corresponding to the perturbed linear system is as follows.

$$\begin{pmatrix} \Delta\phi[n+k] \\ \Delta\phi[n+k-1] \\ \Delta\phi[n+k-2] \\ \vdots \\ \Delta\phi[n] \end{pmatrix} = \begin{pmatrix} -m_1 & -m_1 & \dots & -m_1 & -m_1 \\ 1 & 0 & \dots & 0 & 0 \\ 0 & 1 & \dots & 0 & 0 \\ \vdots & \vdots & \vdots & \vdots & \vdots \\ 0 & 0 & \dots & 1 & 0 \end{pmatrix} \begin{pmatrix} \Delta\phi[n+k-1] \\ \Delta\phi[n+k-2] \\ \Delta\phi[n+k-3] \\ \vdots \\ \Delta\phi[n-1] \end{pmatrix}$$

where $m_1 = f_1'(\phi^*)$. This matrix is the companion matrix for the polynomial expression:

$$\pi(\lambda) = \lambda^{k+1} + \{m_1\}\lambda^k + \{m_1\}\lambda^{k-1} \dots + \{m_1\}\lambda + m_1 \tag{11}$$

The zeros of the polynomial are the eigenvalues of the matrix, and must all have an absolute value less than one, that is, they must lie within the unit circle, in order for the fixed point of the mapping to be stable, which implies that the periodic locking at a fixed delay is also stable in the system from which the PRC was derived. Foss[1] ([22]) was able to derive a simple bound on the slopes of the first order PRC, by first noting that the zeros cross the unit

circle when $m_1 = 1$. By setting λ to1 and $\pi(\lambda)$ to 0 they obtained the lower bound on m_1, such that stability of the perturbed linear system is guaranteed when $-1/k < m_1 < 1$.

III.2 Networks of two neurons

The dynamics of two reciprocally pulsed coupled oscillators has been studied quite extensively ([3], [4], [23], [24]). In this section, we first present the existence and stability criteria for 1:1 phase locked solution with zero phase lag (synchrony) between two reciprocally coupled neurons in terms of their PRCs with arbitrary forms ([12], [25]). We then show that the results for the synchronous firing mode derived by Peskin ([4]) as well as Mirollo and Strogatz ([3]) that assume implicit PRC forms are special cases of the general result.

III. 2.1 1:1 locking with no delay and arbitrary PRC—For any two identical pulse coupled oscillators, synchrony will always exist due to symmetry; the network period of the oscillators remains identical when each oscillator receives an input from the other at phase zero. We give below existence criteria for synchrony between two oscillators that are not necessarily identical ([23], [24]).

By definition (see Fig. 5), for 1:1 phase locking to exist:

$$tr_1[n]=ts_2[n] \tag{12}$$

$$tr_2[n]=ts_1[n+1] \tag{13}$$

where ts_i and tr_i denote the stimulus and recovery intervals of the i^{th} neuron (i=1 or 2), respectively.

Assuming pulsatile coupling, (12) and (13) can be expressed in terms of the phases and the phase resetting, as follows:

$$tr_i[n]=P_i\{(1-\phi_i[n]+f_{1i}(\phi[n])\} \tag{14}$$

$$ts_i[n]=P_i\{\phi[n]+f_{2i}(\phi[n-1])\} \tag{15}$$

where $f_{1i}(\phi)$ and $f_{2i}(\phi)$ represent the first order and second order resetting of the i^{th} neuron, respectively. The intrinsic period of the i^{th} neuron is represented as P_i. The stimulus interval here incorporates the second order resetting due to the input in the previous cycle. If the second order resetting from one input is complete when the next input is received, the assumption of pulsatile coupling remains intact. Higher order resetting cannot be incorporated under this assumption.

The oscillators are assumed to phase lock at the fixed point (ϕ_1^*, ϕ_2^*). The fixed points corresponding to (12) and (13) can be obtained using a graphical method ([15]). Since both the stimulus and recovery intervals are completely determined by the stimulus phase, the

[1]Foss, 1999 ([67]) used the phase resetting curve convention usually used by Mathematicians and opposite to the one used by Biologists (our convention in this article). The translations can be made by using $F(\phi) = -f(\phi)$. The criterion for stability would in this case turn out to be $-1 < F_1'(\phi^*) < 1/k$.

response interval can be considered as a function of the stimulus interval such that tr = g(ts). We can invert the function simply by switching the order of the tr-ts pairs, so ts = g^{-1}(tr). The intersections between the curves $tr_1 = g(ts_1)$ and $ts_2 = g^{-1}(tr_2)$ yield the fixed points.

Substituting for the stimulus and recovery intervals using (14) and (15) in (12) and (13) with appropriate indices, we have:

$$P_1\{1-\phi_1[n]+f_{11}(\phi_1[n])\}=P_2\{\phi_2[n]+f_{22}(\phi_2[n-1])\} \tag{16}$$

$$P_2\{1-\phi_2[n]+f_{12}(\phi_2[n])\}=P_1\{\phi_1[n+1]+f_{21}(\phi_1[n])\} \tag{17}$$

In the neighborhood of ϕ_i^*, $f_{1i}(\phi_i[n]) = f_{1i}(\phi_i^*) + \{f'_{1i}(\phi_i^*)\}\,\Delta\phi_i[n]$ and $f_{2i}(\phi_i[n]) = f_{2i}(\phi_i^*) + \{f'_{2i}(\phi_i^*)\}\,\Delta\phi_i[n]$ where $\Delta\phi_i[n] = \phi_i[n] - \phi_i^*$. $f'_{1i}(\phi_i^*)$ and $f'_{2i}(\phi_i^*)$ are the slopes of the first order and second order PRC at the locking point ϕ_i^*. Substituting for ϕ_1 and ϕ_2 (in terms of the perturbations) in equations (16) and (17) and simplifying produces:

$$\Delta[k+1]=M\,\Delta[k] \tag{18}$$

where $\Delta[k]=[\Delta\phi_1[k], \Delta\phi_2[k]]^T$ with M as the following matrix:

$$\begin{pmatrix} f'_{21} & \frac{P_{0,2}}{P_{0,1}}\left\{f'_{21}-1\right\} \\ \frac{-P_{0,1}}{P_{0,2}}f'_{21}\left\{f'_{11}-1\right\} & \left\{f'_{11}-1\right\}\left\{f'_{12}-1\right\}-f'_{22} \end{pmatrix}$$

The eigenvalues of M are computed from the following characteristic equation:

$$\lambda^2-\lambda\{\{1-f'_{11}(\phi_1^*)\}\{1-f'_{12}(\phi_2^*)\}-f'_{21}(\phi_1^*)-f'_{22}(\phi_2^*)\}+f'_{21}(\phi_1^*)\,f'_{22}(\phi_2^*)=0. \tag{19}$$

Ignoring second order resetting reduces the system to a single eigenvalue

$$\lambda=\{1-f'_{11}(\phi_1^*)\}\{1-f'_{12}(\phi_2^*)\} \tag{20}$$

The above derivation assumes an alternating firing order. To apply the above derivation to the case of synchrony, the eigenvalues from (19) have to be evaluated at (0^+, 1^-) and (1^-, 0^+). The robustness of perturbations from synchrony in which either neuron leads consistently is thereby ensured ([17], [25]).

A slightly different approach to study synchronization utilizes spike time response curves (STRCs) ([12]). A STRC also measures the effects of synaptic perturbations on the timing of subsequent spikes but is measured in terms of time instead of phase and ignores second order resetting. The STRCs were used to predict the change in spike timing between two mutually coupled neurons from one cycle to the next by generating a spike time difference map. This map is just the difference $ts_1[n+1] - ts_1[n]$. They obtain $ts_1[n+1]$ using $\psi_1(\psi_2(ts_1[n]))$, where ψ_j is simply the response time as a function of the stimulus time: $\psi_j(ts) = P_0\{1 + f_{1j}(ts/P_0)\} - ts$. This approach uses the same information and produces the same results as the method described above except that second order resetting is ignored. The zeros of the map are the fixed points, and the stability of the map is same as that given in (20).

A proof similar to the one that resulted in (20) was derived ([26]) for the stability of synchrony for two mutually pulse coupled oscillators ignoring second order resetting. A constant firing order was assured by assuming that the phase transition function $F(\phi) = \phi - f_1(\phi)$ is monotonically increasing and invertible. $F(\phi) > 0$ constrains the slope of the first order PRC as follows: $f_1'(\phi) < 1$. Goel and Ermentrout ([26]) derived a return map that calculates the phase of the second oscillator in the $(n+2)^{nd}$ cycle as a function of that in the n^{th} cycle. The following stability criterion was derived by linearizing the map about the fixed points:

$$\{1 - f_1'(0^+)\}\{1 - f_1'(1^-)\} < 1 \tag{21}$$

Equation (20) reduces to (21) at synchrony for two identical pulse coupled oscillators in which second order resetting is ignored and the firing order is guaranteed to be constant by assuming a monotonically increasing phase transition function.

III.2.2 1:1 locking with no delay and implicit PRC—The earliest work on synchronization of two pulse coupled oscillators was that of Peskin ([4]) who studied synchronization in a network of two mutually excitatory pulse coupled identical leaky integrate and fire neural oscillators. This work can be treated as a special case of the general formulation for two pulse coupled oscillators derived above. The oscillators were characterized by a state variable V(t) whose time course was described by equation (22) and whose value was reset to zero each time it reached a value of one.

$$dV/dt = -\gamma V(t) + S_0 \tag{22}$$

The effect of pulsatile coupling due to the firing of an oscillator was to depolarize the membrane by a fixed amount (ε), or bring the voltage to the threshold value of one, whichever was less. Thus for two oscillators,

$$V_i(t) = 1 \Rightarrow V_j(t) = \min(1, V_i(t) + \varepsilon) \quad \text{for } j \neq i. \tag{23}$$

The form of the synaptic interaction (fixed increment in potential with upper threshold bound) assumed above characterizes the bulk of the physics literature on pulse coupled oscillators, but it is not general enough to capture many forms of synaptic interaction between neurons. The integrate and fire models extensively studied by various investigators can capture the neural dynamics similar to those of type I excitable neurons ([66]) in the sense that phase is advanced by excitations and delayed by inhibition on their respective limit cycles. However, a whole class of excitable neurons i.e. type II ([66]) is ignored by such models. Moreover, the assumption of the fixed increment (or decrement) in the potential function limits the slope of the first order PRC as we show below, and neglects any second order effects, which are sometimes important near synchrony ([17] and [30]). Nonetheless, the integrate and fire models are lot simpler to analyze and hence have been a popular model for investigation. Equation (23) implicitly defines a phase resetting curve because if a perturbation is received at time t, the next spike will be advanced by an amount that can be calculated using the explicit solution for (22) that describes the leaky integrate and fire oscillator. If $V(0) = 0$, then $V(t) = S_0\{1 - e^{-\gamma t}\}/\gamma$. We can solve for the elapsed time to reach a given V(ts) as $ts = \gamma^{-1} \ln(S_0/\{S_0 - \gamma V(ts)\})$. If we denote $A = \ln(S_0/\{S_0 - \gamma\})$, then the time elapsed until $V(t) = 1$, i.e. the intrinsic period of the oscillator, is $T_0 = A/\gamma$. Moreover, the period of the oscillator in the perturbed cycle is: $T_1 = \{-1/\gamma\}\ln(\{S_0 - \gamma\}/\{S_0 - \gamma\,\varepsilon\, e^{A\phi}\})$ for $0 \leq \phi \leq 1$.

Thus, the first order PRC is (see Fig. 6B):

$$f_1(\phi)=\{T_1 - T_0\}/T_0= - \min(|\{\ln(1 - \{\gamma\, \varepsilon\, e^{A\phi}\}/S_0)\}/A|, |\phi - 1|) \quad (24)$$

The negative sign in (24) is necessary to make the PRC sign consistent with the biological convention used in this review. The linear form of the PRC from ϕ = 0.8 to 1.0 results for an excitatory stimulus because there is a causal limit, meaning that an input cannot advance the next spike time to a time before the input was applied, which imposes a limit on the resetting of $\phi - 1$ and necessitates taking the minimum in (24). Starting from, $V_1(0) = 0$ and $V_2(0) = \phi$ ε [0,1], Peskin derived a return map for the phase of the non-firing oscillator (i.e. oscillator 2) immediately after its partner fired (oscillator 1). Each time the map was iterated the roles of the oscillators were reversed. The return map involved computing $\phi_2[n+2]$ in terms of $\phi_2[n]$. For two identical oscillators, the return map has a fixed point at $\phi_2^* = 0.5$ as ε approaches zero. Peskin showed that this fixed point was unstable. This implied that the fixed point repelled trajectories of the oscillators toward synchrony. At synchrony, the coupling term dropped out since each neuron was already at threshold when its partner fired. In this way, synchronization among the oscillators was achieved for every set of initial conditions. A similar result can be achieved by using (20) to calculate the stability of the fixed points directly. For two identical neurons, in order for the absolute value of the eigenvalue in (20) to be less than one, $0 < f'_1(\phi) < 2$. The slope of the PRC given in (24) is:

$$f'_1(\phi)=1/\{1 - S_0\, e^{-A\phi}/\gamma\, \varepsilon\} \quad (25)$$

everywhere except approaching a phase of one where $f'_1(\phi)=1$ (see Fig. 6B). For $S_0\, e^{-A\phi}/\gamma$ $\varepsilon > 0.5$, any fixed point is guaranteed to be unstable. This can be achieved by requiring ε to be sufficiently small. Therefore the antiphase mode observed as ε approaches zero is guaranteed to be unstable. By evaluating $\{1-f'_1(0^+)\}\{1-f'_1(1^-)\}$, (20) can also be used to prove the stability of synchrony. Since we already know that $f'_1(1^-) = 1$, $\lambda=0$ and hence synchrony is guaranteed to be stable regardless of the value of $f'_1(0^+)$. The proof in terms of (20) is a novel proof that indicates that synchrony is locally stable, whereas the original proof of Peskin was global in that it relied on a globally repellent fixed point, distinct from the one at synchrony, to stabilize synchrony.

Mirollo and Strogatz ([3]) generalized the results obtained by Peskin ([4]) to any two pulse coupled oscillators. Instead of assuming that the state variable (i.e. the membrane potential V) evolved according to (22), they assumed that time course of the function describing the evolution was a smooth monotonically increasing and concave down function with $V'(t) > 0$, $V''(t) < 0$ and $V(0)=V(1)=0$, as it is for the leaky integrator and fire model neuron (see Fig. 6A). Since the interaction between the two oscillators was assumed to be pulsatile, the firing of one oscillator was assumed to depolarize the other by an amount ε (see Fig. 6A) or pull it up to the firing threshold, whichever was less.

Again, this implicitly defines a PRC, allowing a return map to be formulated. Peskin's proof assumed that ε and γ were small. For identical and identically coupled two leaky integrate and fire model neurons Mirollo and Strogatz found that for almost all initial conditions and for all ε, $\gamma > 0$ synchrony was a solution. The return map was proved to have a unique unstable fixed point based on the assumption of concavity. Thus, all the oscillators were globally repelled toward synchrony. The disappearance of the coupling term allowed the synchronized state to persist. The proof given above for Peskin's example holds for local synchrony in the more general case of Mirollo and Strogatz because once again $f_1(\phi)= \phi - 1$ at phase approaching one. The key observation is that the slope of one near a phase of one

stabilizes synchrony. The same argument can be applied to non-leaky integrators in which the concavity requirement is relaxed ([56]). The slope for the initial portion of such a PRC is zero, meaning any attractors with a locking point in this region must be neutrally stable by (20) since $1-f_1'(\phi) = 0$, whereas the form of the PRC still requires a slope of one at phase equal to one, stabilizing synchrony and conferring upon it nearly global attractiveness (see Fig. 6B).

III.2.3 1:1 locking with delay and implicit PRC—Mirollo and Strogatz ([3]) proved that synchronization with zero phase difference between two pulse coupled oscillators was globally attracting for leaky integrate and fire type oscillators in response to excitation under some assumptions. Ernst et al. ([5], [6]) extended those results to include the effects of inhibition as well as pulse conduction delays up to half the intrinsic period. As in [3], the state variable, V(t), was assumed to be monotonically increasing $V'(t) > 0$ and concave down $V''(t) < 0$. Once again, the synaptic interactions were assumed to increment the potential by a fixed amount ε, which could be positive for excitation or negative for inhibition, and again implicitly defined a form for the PRC. Under the assumptions given, an excitation applied at a later phase will advance the phase more than one given at an earlier phase, resulting in a negative slope for the PRC unless the causality limit is reached such that an immediate spike results. In the latter region, we have already shown that a positive PRC slope equal to one results. Ernst et al. ([5]) found that for mutual excitation and small delays, at all coupling strengths phase locking with a time lag between the two neurons equal to the delay was found to be always stable whereas synchrony was not. In the case in which the time lag is equal to the delay, one neuron (but not the other) induces its partner to fire immediately. Therefore, the slope at the locking point for the partner is one, which as we have previously stated, stabilizes the mode regardless of the slope at the locking point for the other neuron. On the other hand, for synchrony and small delays, the locking point is at a phase equal to the normalized delay, and both slopes are negative. Thus the results apply only to cases in which the slopes of the PRC follow a similar pattern. Also, there is no second order resetting by assumption; the presence of such resetting can also alter the stability results. Since the slope of the PRC for inhibition is opposite to that for excitation and unbounded by causality, under the restrictive assumptions for the form of the PRC described above, the slope of the PRC for inhibition is generally positive, and was found to produce global synchrony for many delays and conductance values. A positive PRC slope at the locking point is not by itself sufficient to guarantee stability. However, the monotonicity of V(t) guarantees that a fixed increment or decrement ε in V(t) at two distinct old phases (before an input) preserves the order of the new phases (after an input) (see Fig. 6A), which implies a monotonically increasing phase transition function that maps the old phase onto the new phase. As we showed above, this guarantees that the slope of the first order PRC is less than one, so inhibition is stable for arbitrary inhibitory coupling strength.

III.2.4 1:1 locking with delays and arbitrary PRC—A more general approach to studying pulse coupled oscillators with conduction delays would involve PRCs that are implicit and abstract. Pervouchine et al. ([13]) used a method that is very similar to the pulse coupled phase resetting methods based on the stimulus and response times, except that second order resetting was neglected. For two identical, identically coupled oscillators firing in alternation with identical short delays (δ), the spike time difference is $ts_1[n+1] = ts_1[n]$, where $ts_1[n+1] = \psi_1(\psi_2(ts_1[n]))$, and the map ψ_j is simply the response time as a function of the stimulus time: $\psi_j(ts) = P_0\{1 + f_{1j}(\{ts+\delta\}/P_0)\} - ts - \delta$, where P_0 is the intrinsic period of the i^{th} neuron and f_{1i} is the first order resetting of the i^{th} neuron. The zeros of the map give the fixed points and stability criterion for this map is the same as that given in (20).

Stability results for all possible firing patterns in two bidirectionally pulse coupled oscillators with conduction delays were derived by Woodman and Canavier ([27]) using

only the PRCs' of the concerned oscillators. Fig. 7A illustrates one possible firing pattern. Here k cycles are assumed to occur before the firing of a spike in neuron 1 affects the timing of the next spike in neuron 1 via the feedback loop through neuron 2. If j_2 is defined as the number of spikes in neuron 2 that occur during the delay period δ_1 and j_1 as the number of spikes in neuron 1 that occur during the delay period δ_2 then $k= (j_1 + j_2 +1)$. The corresponding firing map based on the stimulus and recovery intervals is:

$$ts_1[n+k-1]=tr_2[n+j_2-1]+\delta_1+\delta_2-\sum_{i=0}^{k-2}(ts_1[n+i]+tr_1[n+i]) \tag{26}$$

$$ts_2[n+k-1]=tr_1[n+j_1]+\delta_1+\delta_2-\sum_{i=0}^{k-2}(ts_2[n+i]+tr_2[n+i]) \tag{27}$$

The quantities on the left side are written in terms of earlier intervals. The summation is only applied for k greater than two. Surprisingly, this exact expression generalizes to all firing patterns (for example see Fig. 7B). To derive the stability results the techniques that were previously used to write the expressions of the firing map in terms of phase resetting is applied along with linearization about the appropriate fixed points to produce the general results ([27]).

III.2.5 N:N locking with no delay and arbitrary PRC—Firing orders that are not constant from cycle to cycle were considered by Maran and Canavier, ([15]) and Oh and Matveev ([16]) in a network of two pulse coupled oscillators with no conduction delays and arbitrary PRCs. Maran and Canavier ([15]) successfully predicted 1:1 and 2:2 phase locked modes in heterogeneous networks using only the component first order and second order PRCs. Separate existence and stability criteria for the 2:2 mode in which the firing order was preserved and for those in which the leading neuron switches on each cycle (termed as "leap-frog" by G.B. Ermentrout or "leader-switching" by Acker et al. ([12])) were derived (see Fig.8). Both criteria reduce to

$$ts_{11}=tr_{21};P_1\{\phi_{11}[n]\}=P_2\{1-\phi_{22}[n-1]+f_{12}(\phi_{22}[n-1])\} \tag{28}$$

$$ts_{12}=tr_{22};P_1\{\phi_{12}[n]-\phi_{11}[n]+f_{11}(\phi_{11}[n])\}=P_2\{1+f_{22}(\phi_{21}[n-1])+f_{22}(\phi_{22}[n-1])\} \tag{29}$$

$$ts_{21}=tr_{11};P_2\{\phi_{21}[n]\}=P_1\{1-\phi_{12}[n]+f_{11}(\phi_{12}[n])\} \tag{30}$$

$$ts_{22}=tr_{12};P_2\{\phi_{22}[n]-\phi_{21}[n]+f_{12}(\phi_{21}[n])\}=P_1\{1+f_{21}(\phi_{11}[n])+f_{21}(\phi_{12}[n])\} \tag{31}$$

A stable leapfrog 2P mode is predicted if the roots of the following characteristic equation of the linearized system have an absolute value less than 1:

$$\lambda^2 - \lambda \{f'_{22}(\phi_{21}^*)(f'_{11}(\phi_{12}^*) - 1) + f'_{21}(\phi_{11}^*)(f'_{12}(\phi_{22}^*) - 1) + \{f'_{21}(\phi_{12}^*) + (1 - f'_{12}(\phi_{21}^*))(f'_{11}(\phi_{12}^*) - 1)\}\{f'_{22}(\phi_{22}^*) + (1 - f'_{11}(\phi_{11}^*))(f'_{12}(\phi_{22}^*) - 1)\}\} + f'_{21}(\phi_{11}^*)f'_{22}(\phi_{21}^*)(1 - f'_{11}(\phi_{12}^*))(1 - f'_{12}(\phi_{22}^*)) = 0. \quad (32)$$

The stability results for the two 2:2 modes are different, but if second order resetting is ignored; they both reduce to the following form, which is an intuitive extension of (20).

$$\lambda = (1 - f'_{11}(\phi_{11}^*))(1 - f'_{11}(\phi_{12}^*))(1 - f'_{12}(\phi_{21}^*))(1 - f'_{12}(\phi_{22}^*)). \quad (33)$$

However, it was sometimes required to account for second order resetting in order to obtain accurate predictions.

Oh and Matveev ([16]) provided a geometric description of the “leap-frog” network activity in two identical and identically pulse coupled Morris-Lecar model neurons ([29]) with inhibitory synapses near a type-I membrane excitability regime ([55] and [75]). They showed that the synchronous firing mode was lost when the inhibitory coupling strength was increased through a period-doubling cascade (see Fig. 2A). Consequently, mode-locked states with alternation in the firing order of the two cells i.e. the leap-frog mode was observed. The reason for the change in firing order was demonstrated using phase-plane analysis. Inhibition from the lagging cell was sufficient to transiently place the leading cell below the excitability threshold, in a region that was not on the original limit cycle. A negative phase was assigned to this region because the time to the next spike at the phase was greater than an unperturbed period. The phase delay is greater than the interval that separated the firing of the two neurons allowing the lagging cell to become the leading cell on the next cycle.

Gerstner ([65]) examined non-leaky integrate and fire oscillators (the potential function V(t) is monotonically increasing in a linear rather than concave down fashion) in which the coupling again takes the form of a bounded fixed increment in the potential function. This defines an implicit PRC which could be used to apply the results for arbitrary PRC to this case as well. Interestingly, Gerstner identified and analyzed phase locking for N pulse coupled inhibitory neurons with delay in which every other cycle was delayed by the receipt of two delayed pulses from every other oscillator, but the intervening cycles were not delayed, resulting in a 2:2 mode for two neurons and an analogous mode for larger networks.

III.2.6 N:1 locking with no delay and arbitrary PRC—Cross-frequency synchronization (a. k. a N:1 harmonic locking) between two reciprocally pulse coupled oscillators with no delay was investigated by Canavier et al. ([28]). The focus was on N:1 phase locked modes in which the fast oscillator (F) received an input every N^{th} cycle from the slow oscillator (S) at a constant phase within that N^{th} cycle (see Fig. 9). The corresponding firing map is:

$$ts_F[m]=tr_S[m] \tag{34}$$

$$tr_{F1}[m+1]=ts_{S1}[m+1] \tag{35}$$

$$tr_{F2}[m+1]=ts_{S2}[m+1] \tag{36}$$

The time elapsed between the most recent spike in the faster neuron and the time at which it receives the input from the slower neuron is ts_F. The time elapsed between the receipt of the last (N^{th}) input in a given slow neuron cycle and the next spike in the slow neuron is tr_S. The time elapsed between when the fast neuron receives an input and when the fast neuron next fires is tr_{F1}. The time elapsed between when the slower neuron fires and when it receives the first input from the faster neuron at a phase of ϕ_{S1} is ts_{S1}. The remaining (N−1) cycles of the fast neuron make up tr_{F2}. The time elapsed between the arrival of the first input in the slow neuron and the receipt of the N^{th} input at a phase of ϕ_{SN} is ts_{S2}.

Substituting for the stimulus and recovery intervals in (34)–(36) we get the following periodicity criteria:

$$P_F\,\phi_F[m]=P_S\{1-\phi_{SN}[m]+f_{1S}(\phi_{SN}[m])\} \tag{37}$$

$$P_F\,\{1-\phi_F[m]+f_{1F}(\phi_F[m])\}=P_S\{\phi_{S1}[m+1]+f_{2S}\,(\phi_{SN}[m])\} \tag{38}$$

$$P_F\,\{N-1+f_{2F}(\phi_F[m])\}=P_S\left\{\phi_{SN}[m+1]-\phi_{S1}[m+1]+\sum_{j=1}^{N-1} f_{1S}\,(\phi_{Sj}[m+1])\right\} \tag{39}$$

Solving for the phases in terms of ϕ_{SN} using (37) and (38), we have:

$$\phi_F[m]=(P_S/P_F)\,\{1-\phi_{SN}[m]+f_{1S}\,(\phi_{SN}[m])\} \tag{40}$$

$$\phi_{S1}[m+1]=(P_F/P_S)\,\{1-\phi_F[m]+f_{1F}(\phi_F[m])\}-f_{2S}\,(\phi_{SN}[m]) \tag{41}$$

As in section III.2.1, for the i^{th} neuron, in the neighborhood of ϕ_i^*, $f_{1i}(\phi_i[n]) = f_{1i}(\phi_i^*) + \{f'_{1i}(\phi_i^*)\}\,\Delta\phi_i[n]$ and $f_{2i}(\phi_i[n]) = f_{2i}(\phi_i^*) + \{f'_{2i}(\phi_i^*)\}\,\Delta\phi_i[n]$ where $\Delta\phi_i[n] = \phi_i[n] - \phi_i^*$. Therefore, (40) and (41) in terms of perturbations turn out to be:

$$\phi_F^*+\Delta\phi_F[m]=(P_S/P_F)\,\{1-\phi_{SN}^*-\Delta\phi_{SN}[m]+f_{1S}\,(\phi_{SN}^*)+f'_{1S}\,(\phi_{SN}^*)\,\Delta\phi_{SN}[m]\} \tag{42}$$

$$\phi_{S1}{}^{*}+\Delta\phi_{S1}\,[m+1]=(P_F/P_S)\,\{1-\phi_F{}^{*}-\Delta\phi_F[m]+f_{1F}(\phi_F{}^{*})+f'_{1F}\,(\phi_F{}^{*})\,\Delta\phi_F[m]\}-f_{2S}\,(\phi_{SN}{}^{*})-f'_{2S}\,(\phi_{SN}{}^{*})\Delta\phi_{SN}[m] \tag{43}$$

Cancelling the steady state terms from both sides of (42) and (43), we get:

$$\Delta\phi_F\,[m]=(P_S/P_F)\,\{f'_{1S}(\phi_{SN}{}^{*})-1\}\Delta\phi_{SN}\,[m] \tag{44}$$

$$\Delta\phi_{S1}\,[m+1]=(P_F/P_S)\{f'_{1F}\,(\phi_F{}^{*})-1\}\Delta\,\phi_F[m]-f'_{2S}\,(\phi_{SN}{}^{*})\Delta\phi_{SN}\,[m] \tag{45}$$

Substituting for $\Delta\phi_F\,[m]$ in (45) using (44), we have:

$$\Delta\phi_{S1}\,[m+1]=\{\{f'_{1F}(\phi_F{}^{*})-1\}\,\{f'_{1S}(\phi_{SN}{}^{*})-1\}-f'_{2S}(\phi_{SN}{}^{*})\}\Delta\phi_{SN}\,[m] \tag{46}$$

The $\Delta\phi_{Sj}\,[m+1]$ can be written in terms of $\Delta\phi_{S1}\,[m+1]$ and $\Delta\phi_F\,[m]$:

$$\phi_{S2}[m+1]=\phi_{S1}[m+1]-f_{1S}(\phi_{S1}[m+1])+P_F/P_S\{1+f_{2F}(\phi_F\,[m])\} \tag{47}$$

$$\phi_{Sj}[m+1]=\phi_{S(j-1)}[m+1]-f_{1S}(\phi_{S(j-1)}[m+1])+P_F/P_S \tag{48}$$

The linearized expressions about the steady state fixed points are:

$$\phi_{S2}{}^{*}+\Delta\phi_{S2}[m+1]=\phi_{S1}{}^{*}+\Delta\phi_{S1}[m+1]-f_{1S}(\phi_{S1}{}^{*})-f'_{1S}(\phi_{S1}{}^{*})\Delta\phi_{S1}[m+1]+P_F/P_S\,\{1+f_{2F}(\phi_F{}^{*})+f'_{2F}(\phi_F{}^{*})\Delta\phi_F[m]\} \tag{49}$$

$$\phi_{Sj}{}^{*}+\Delta\phi_{Sj}[m+1]=\phi_{S(j-1)}{}^{*}+\Delta\phi_{S(j-1)}[m+1]-f_{1S}(\phi_{S(j-1)}{}^{*})-f'_{1S}(\phi_{S(j-1)}{}^{*})\Delta\phi_{S(j-1)}[m+1]+P_F/P_S \tag{50}$$

Cancelling the steady state terms from both sides of (49) and (50), we get:

$$\Delta\phi_{S2}[m+1]=\{1-f'_{1S}(\phi_{S1}{}^{*})\}\Delta\phi_{S1}[m+1]+(P_F/P_S)f'_{2F}(\phi_F{}^{*})\Delta\phi_F[m] \tag{51}$$

$$\Delta\phi_{Sj}[m+1]=\{1-f_{1S}(\phi_{S(j-1)}{}^{*})\}\Delta\phi_{S(j-1)}[m+1] \tag{52}$$

The recursive dependence of the $\Delta\phi_{Sj}$ on $\Delta\phi_{S1}[m+1]$ and $\Delta\phi_F[m]$ gives rise to the two summation terms containing Π in the expression for the eigenvalue.

For j>2, from (52) we have:

$$\Delta\phi_{Sj}[m+1]=\prod_{k=1}^{j-1}\{1-f'_{1S}(\phi_{Sk}^{*})\}\,\Delta\phi_{S1}[m+1]+\left(\frac{P_F}{P_S}\right)\prod_{k=2}^{j-1}\{1-f'_{1S}(\phi_{Sk}^{*})\}f'_{2F}(\phi_F^{*})\,\Delta\phi_F[m] \tag{53}$$

Substituting for $\Delta\phi_{S1}\,[m+1]$ and $\Delta\phi_F\,[m]$ in (53) using (44) and (46), we obtain:

$$\Delta\phi_{Sj}[m+1]=\{\prod_{k=1}^{j-1}\{1-f'_{1S}(\phi^*_{Sk})\}\{\{f'_{1F}(\phi^*_F)-1\}\{f'_{1S}(\phi^*_{SN})-1\}-f'_{2S}(\phi^*_{SN})\}+f'_{2F}(\phi^*_F)\{f'_{1S}(\phi^*_{SN})-1\}\prod_{k=2}^{j-1}\{1-f'_{1S}(\phi^*_{Sk})\}\}\Delta\phi_{SN}[m] \quad (54)$$

Solving for ϕ_{SN} [m+1] in (39), we obtain:

$$\phi_{SN}[m+1]=\phi_{S1}[m+1]-f_{1S}(\phi_{S1}[m+1])-\sum_{j=2}^{N-1}f_{1S}(\phi_{Sj}[m+1])+\left(\frac{P_F}{P_S}\right)\{N-1+f_{2F}(\phi_F[m])\} \quad (55)$$

Linearizing the above equation about the fixed points we have:

$$\phi^*_{SN}+\Delta\phi_{SN}[m+1]=\phi^*_1+\Delta\phi_{S1}[m+1]-f_{1S}(\phi^*_{S1})-f'_{1S}(\phi^*_{S1})\Delta\phi_{S1}[m+1]-\sum_{j=2}^{N-1}\{f_{1S}(\phi^*_{Sj})+f'_{1S}(\phi^*_{Sj})\Delta\phi_{Sj}[m+1]\}+\left(\frac{P_F}{P_S}\right)\{N-1+f_{2F}(\phi^*_F[m])+f'_{2F}(\phi^*_F)\Delta\phi_F[m]\} \quad (56)$$

Cancelling the steady state terms from both sides of (56), we get:

$$\Delta\phi_{SN}[m+1]=\{1-f'_{1S}(\phi^*_{S1})\}\Delta\phi_{S1}[m+1]-\sum_{j=2}^{N-1}f'_{1S}(\phi^*_{Sj})\Delta\phi_{Sj}[m+1]+\left(\frac{P_F}{P_S}\right)\{f'_{2F}(\phi^*_F)\Delta\phi_F[m]\} \quad (57)$$

Substituting for $\Delta\phi_{S1}$ [m+1] from (46), $\Delta\phi_{Sj}$[m+1] from (54) and for $\Delta\phi_F$ [m]from (44) into (57), we get:

$$\Delta\phi_{SN}[m+1]=\{\{\{1-f'_{1S}(\phi^*_{S1})\}\{f'_{1F}(\phi^*_F)-1\}\{f'_{1S}(\phi^*_{SN})-1\}-f'_{2S}(\phi^*_{SN})\}-\sum_{j=2}^{N-1}\{f'_{1S}(\phi^*_{Sj})\{\{f'_{1F}(\phi^*_F)-1\}\{f'_{1S}(\phi^*_{SN})-1\}-f'_{2S}(\phi^*_{SN})\}\prod_{k=1}^{j-1}\{1-f'_{1S}(\phi^*_{Sk})\}\}+\sum_{j=2}^{N-1}\{f'_{1S}(\phi^*_{Sj})f'_{2F}(\phi^*_F)\{f'_{1S}(\phi^*_{SN})-1\}\Big] \quad (58)$$

Simplifying, we obtain ([28]):

$$\Delta\phi_{SN}[m+1]=\lambda\,\Delta\phi_{SN}[m] \quad (59)$$

where

$$\lambda = f'_{2F}(\phi^*_F)\{f'_{1S}(\phi^*_{SN}) - 1\} + \sum_{j=2}^{N-1}\{f'_{1S}(\phi^*_{Sj})\, f'_{2F}(\phi^*_F)\{f'_{1S}(\phi^*_{SN}) - 1\}\prod_{k=2}^{j-1}\{1 - f'_{1S}(\phi^*_{Sk})\}\} + \{\{f'_{1F}(\phi^*_F) - 1\}\{f'_{1S}(\phi^*_{SN}) - 1\} - f'_{2S}(\phi^*_{SN})\}\{1 - f'_{1S}(\phi^*_{S1})\} - \sum_{j=2}^{N-1} f'_{1S}(\phi^*_{Sj})\prod_{k=1}^{j-1}\{1 - f'_{1S}(\phi^*_{Sk})\}\} \quad (60)$$

For N=2, the summation terms drop out; for N=3 the product term $\prod_{k=2}^{j-1}\{1 - f'_{1S}(\phi^*_{Sk})\}$ drops out. For stable N:1 phase locked mode $|\lambda| < 1$. This PRC based approach correctly predicted 2:1, 3:1, 4:1 and 5:1 phase locked modes ([28]).

III.3 Ring networks and chains

III.3.1 Unidirectional ring—Networks in which each oscillator receives an input from one other oscillator and delivers an input to one other oscillator are referred to as ring networks. In networks involving more than two oscillators the coupling between the oscillators in a ring is by definition unidirectional (see Fig. 11). Dror et al. ([32]) considered the case of a unidirectional ring of pulse coupled oscillators with excitatory or inhibitory synapses. In this case, each oscillator received exactly one input per cycle. The oscillators in a ring circuit tend to phase lock where each oscillator fires with a fixed frequency and fixed phase difference. At steady state 1:1 phase locked mode:

$$P_i\{1 + f_{1i}(\phi_i^*)\} = P_e \quad (61)$$

where P_i represents the intrinsic period of the oscillators, P_e represents the common entrained period of the N neural oscillators and $f_{1i}(\phi_i^*)$ represents the first order resetting of the i^{th} oscillator. If $ts_i[n]$ denotes the difference in firing times of adjacent oscillators in the n^{th} cycle of a ring, then at steady state (see Fig.11):

$$ts_1[n] + ts_2[n] + \ldots + ts_{N-1}[n] + ts_N[n] = kP_e \quad (62)$$

where $ts_i[n] = P_i\{\phi_i^* + \Delta\phi_i[n]\}$ for i=1,2,…N and k ε [0, N −1]. Each value of k produces a different firing order. (N + k −1) cycles elapse before the feedback due to a spike in a particular oscillator propagates back to that oscillator, similar to the integer k in Foss and Milton ([22]) (see III. 1.2). Let $\Delta\phi_i[n+1]$ denote the change in the phase of the i^{th} oscillator in the $(n+1)^{st}$ cycle. The vector $\Delta\phi[n+1]$ in a ring of N coupled oscillators using PRCs is fully described by the (N−1) state variables $\Delta\phi_i[n+1]$ where i ε [1, N −1]. Here, unlike the case of the two coupled oscillators, we have: $\Delta\phi[n+1] = A\,\Delta\phi[n]$ where A is the Jacobian matrix of the discrete-time system determined by the PRCs ([32]). The matrix A has been worked out by Dror et al. ([32]) where second order resetting was ignored and time was used instead of the phase variable. The matrix A is unchanged for two non-identical oscillators and is given in [25] for heterogeneous rings of two and three including the second order terms. The matrix A is distinct for each assumed firing order.

In the case of N-ring coupled oscillators the eigenvalues of the matrix A determine the stability of the system given the values of $f_{1i}(\phi_i^*)$ for i=1,2,…N. If λ_{max} denotes the maximum eigenvalue and if $|\lambda_{max}| < 1$ stability is guaranteed. These existence and stability

criteria predict the activity of model neural networks accurately as long as the duration of the coupling is short compared to the period ([7], [8], [10]).

III.3.2 Bidirectional rings and chains—A network of N pulse coupled oscillators with coupling between nearest neighbors along a single dimension such that $(N+1)^{st}$ oscillator is identified with the 1^{st} oscillator and N^{th} oscillator is identified with the 0^{th} oscillator is referred to as a bidirectional ring. Phase locking between pulse coupled oscillators with such geometry was studied by Goel and Ermentrout ([26]) in phase reduced model using implicit PRCs as the coupling. For a bidirectional ring in which N = 2 or 3 as well as for a linear bidirectional chain in which N = 2, the results for an all to all system apply, see III.4.1. Goel and Ermentrout did not find a sufficient condition for synchrony in bidirectional rings or chains due to the permutations of the firing order than can result from a small perturbation. Under the restrictive assumptions that inhibition produces only phase delays resulting from a fixed decrement of a monotonically increasing concave down potential function, Timme et al. ([57] and [58]) found that synchrony in pulse coupled networks with arbitrary coupling strength and connectivity was always stable (see III.4.1). Goel and Ermentrout ([26]) pointed out that although symmetry guarantees the existence of synchrony in all to all networks and bidirectional rings comprised of identical oscillators, for a bidirectional linear chain the additional constraint must be imposed that two simultaneous inputs must have the same effect as a single one at a phase of zero to keep the period of the end oscillators the same as that of the middle oscillators; they suggested the condition $f_1(0) = 0$. In the wave solution (or splay) in a bidirectional ring, the interval between the firing of successive oscillators is a constant ts_i. For identical oscillators, the phase ϕ_1^* at which the first input is received in each cycle is ts_1 divided by the intrinsic period, and the second and last input is received at $\phi_2^*=(N-1)\phi_1^*-f_1(\phi_1^*)$. Goel and Ermentrout found that stability of the splay mode in the bidirectional ring is guaranteed if the roots of the following characteristic equation are all less than one:

$$\lambda^N+\{1-f_1'(\phi_2^*)\}\{\lambda^{N-1}+\cdots+\lambda\}+\{1-f_1'(\phi_1^*\}\{1-f_1'(\phi_2^*)\}=0 \quad (63)$$

under the assumption of a monotonically increasing phase transition function.

III.4. All to all N neuron networks

III.4.1 Synchrony

III.4.1.1 Synchrony with no delay and arbitrary PRC: In a network of all to all identical, identically connected neurons as considered in Achuthan and Canavier ([17]) synchronous firing mode exists due to symmetry; in the fully synchronous state, each neuron receives simultaneous inputs from (N−1) other neurons so their phase locked periods remain identical. In order to be stable, global synchrony must be robust to small perturbations. Goel and Ermentrout ([26]) assumed a perturbation in which the firing of all neurons was separated such that they fire sequentially without changing order, then determined the PRC slopes that allowed convergence back to synchrony. In their scheme, all oscillators were absorbed into a synchronous cluster simultaneously, so the effects of sequential absorptions were not considered. Such a proof is better suited to the splay mode, as described in the next section. On the other hand, Achuthan and Canavier ([17]) developed a criterion for robustness of global synchrony to the perturbation of a single neuron from global synchrony, resulting in a single neuron coupled to a population of (N−1) neurons (see Fig. 12A). The stability criterion given below is a straightforward extension of the proof for the case of two neurons ([24], [32]). The effects of the (N−1) neurons within a cluster on each other are ignored below, and the large cluster is treated as a single oscillator whose conductance is (N −1) times that of the single neuron.

The main idea is to use a stability criterion derived for the perturbed firing order, but then to apply it at synchrony using the left and right limits of the phases at one and zero. A new proof is not required, we simply apply (20) to a reciprocally coupled heterogeneous system in which one oscillator is a cluster of (N−1) oscillators and the other is a single oscillator. Thus the coupling from the cluster to the single oscillator is (N−1) times as strong as the coupling from the single oscillator to the cluster.

The corresponding characteristic polynomial corresponding is:

$$\lambda^2-\lambda\{\{1-f'_{1,1}(\phi_1^*)\}\{1-f'_{1,N-1}(\phi_{N-1}^*)\}-f'_{2,1}(\phi_1^*)-f'_{2,N-1}(\phi_{N-1}^*)\}+f'_{2,1}(\phi_1^*)\,f'_{2,N-1}(\phi_{N-1}^*)=0. \quad (64)$$

In order to actually apply the criterion, one can measure the PRC for the cluster of (N−1) neurons directly, or simply assume that the PRC of the cluster can be approximated by that of a single neuron as in [17]. The stability criterion is then applied twice to consider perturbations in which the single neuron either leads or lags the larger cluster i.e. once at $\phi_1^* = 0^+$ and $\phi_{N-1}^* = 1^-$, and again at $\phi_1^* = 1^-$ and $\phi_{N-1}^* = 0^+$ (see Fig.12A). Often, $f'_{1,i}(1^-)$ and $f'_{2,i}(0^+)$ are near zero, for i=1 and (N−1), and if the PRC is flat in those regions, the expression reduces to a single eigenvalue for each evaluation: $\lambda = 1 - f'_{1,1}(0^+) - f'_{2,N-1}(1^-)$ and $\lambda = 1 - f'_{1,N-1}(0^+) - f'_{2,1}(1^-)$. $f'_{1,i}(0^+) = f'_{2,i}(1^-)$ for i = 1 and (N−1) because they measure the same quantity, namely; the resetting in the next cycle when the perturbation occurs at the time of action potential initiation. Thus, we obtain the following eigenvalue twice: $\lambda = 1 - f'_{1,1}(0^+) - f'_{1,N-1}(1^-)$, from which it is easy to see that negative slopes are destabilizing, as are large positive slopes. On the other hand, $f'_{1,i}(1^-)$ is not small in all cases, but rather approaches one for strong excitation that evokes an action potential almost immediately. This is the case for the examples from the work of Peskin ([4]) and Mirollo and Strogatz ([3]) discussed below.

III.4.1.2 Synchrony with no delay and implicit PRC: Peskin's synchrony proof ([4]) derived for two mutually excitatory pulse coupled leaky intergrate and fire neurons can be extended to N neurons by using the coupling strength parameter ε' instead of ε with ε' = ε/ N where the membrane potential evolved according to (22). Mirrollo and Strogatz ([3]) also proved that synchronization in a population of excitatory all to all pulse coupled leaky integrate and fire neurons was feasible. They assumed that the function representing the evolution of the oscillators was monotonically increasing as well as concave down. Their basic idea was to show as the system evolved oscillators clumped together to form groups. Larger groups tended to absorb small ones until one single group remained. The first part of their proof showed that for almost all initial conditions, an absorption occurred in finite time. The second and final part exhibited that the set of initial conditions that lived for ever without leading to synchrony after a certain number of absorptions was of measure zero.

The splay mode in which individual neurons or subclusters fire sequentially in the N neuron case is analogous to the antiphase mode. In general, the splay modes are unlikely to be stable for the same reason that antiphase is unstable in the case of two neurons, namely that under their assumptions the slope of the PRC is negative everywhere except near one, which would tend to destabilize any splay mode. The positive slopes near one would lead to synchronization. Second order resetting is zero by definition under the assumptions of Peskin ([4]) and of Mirollo and Strogatz ([3]), and the same argument that guarantees the stability of the synchronous mode for two neurons guarantees the stability of the synchronous mode for the N neuron cases by (64) above because the slope at phase equal to one is one, resulting in a zero eigenvalue whether the single neuron or the cluster leads. The stability of the globally synchronous solution is guaranteed by the form assumed for the

PRC. Global synchrony is not guaranteed to be a stable solution for all networks of pulse coupled oscillators with mutual excitation ([17]).

III.4.1.3 Synchrony with delay and implicit PRC: Timme et al. ([57],[58]) made assumptions similar to those of Ernst et al. ([5]) allowing for small delays in a network of N oscillators. They constructed a stroboscopic map around global synchrony that considered all possible firing orders as perturbations of the synchronous state. Under the assumptions that the synaptic interactions take the form of a fixed increment in potential with an upper bound and that the potential function V(t) be strictly increasing (V'(t)>0) and concave down V''(t) <0, they showed that the globally synchronous state was always stable for mutually inhibitory neurons with arbitrary coupling strength and arbitrary connectivity (includes all to all, rings and chains). The results are a consequence of the restrictive assumptions, because examples of networks with inhibitory pulse coupling can be found that do not stably synchronize ([17]). In addition, if $f_1'(0)\neq 0$, then synchrony may not exist in an arbitrarily connected network (see III.3.2).

III.4.2 Splay modes—The mode in which the pulse coupled oscillators fire in a sequential manner once per cycle such that no two fire simultaneously is referred to as the splay firing mode. Goel and Ermentrout ([26]) derived the stability proof for synchrony based on the map given in Fig. 12B. This proof was generalized to the splay firing pattern by Achuthan and Canavier ([17]). They used the expressions for the transient values of the stimulus intervals indexed by spike k to form a discrete coupled map of the (N−1) phases at which inputs are received when the reference neuron spikes. We first present this proof for stability assuming that all the oscillators are identical and that the phase transition function ($F(\phi)=\phi - f_1(\phi)$) is monotonically increasing.

Let the phases of the oscillators immediately before oscillator N fires be: $1 > \phi_{N-1} > \phi_{N-2} > \ldots > \phi_2 > \phi_1 > 0$. The phase of the firing oscillator ϕ_N is taken to be 1 in the k^{th} cycle and the oscillators are re-indexed on every cycle so that only (N−1) variables are required. Considering only first order resetting due to a single input and ignoring higher order resetting, we obtain expressions for the phase immediately after a perturbation ($\bar{\phi}$) in terms of the phase immediately before the perturbation (ϕ): $\bar{\phi}_N = 0$ and $\bar{\phi}_i = \phi_i - f_i(\phi_i) = F(\phi_i)$ for i=1,…, (N−1). Since the phase transition function is monotonically increasing we have $\bar{\phi}_{N-1} \geq \bar{\phi}_{N-2} \geq \ldots \geq \bar{\phi}_1$. The next step is to advance all of the phases until just before the next neuron fires, but keeping the numbering such that the neuron that just fired as oscillator N in cycle k is now oscillator 1 in cycle (k+1), oscillator 1 is now 2, and so on (see Fig. 12B). The phase ϕ_1 [k+1] in the stimulus interval ts_1 is equal to the normalized recovery interval $1 - \phi_{N-1}$ i.e.:

$$\phi_1\,[k+1]=1-\bar{\phi}_{N-1}=1-\phi_{N-1}[k]+f_1(\phi_{N-1}[k]). \tag{65}$$

Each phase can then be updated to the next firing time by adding ϕ_1 [k+1] to the phase after the previous input and increasing the index by one as in Fig. 12B.

$$\phi_{i+1}\,[k+1]=\bar{\phi}_i[k]+\phi_1\,[k+1]=\phi_i[k]-f_1(\phi_i[k])+\phi_1\,[k+1] \tag{66}$$

for i=1 to (N−2). In the above equations we can assume a perturbation $\Delta\phi_i[k]$ about a fixed point ϕ_i^* such that $\phi_i[k] = \phi_i^* + \Delta\phi_i[k]$ for i=1,…, (N−1); where ϕ_i^* is the steady state fixed point. After linearizing the PRCs as before and cancelling the steady state terms from both sides of (65) and (66) we obtain the following linear system:

$$\Delta\phi_{N-1}[k+1]=\{f'_1(\phi_{N-1}{}^*)-1\}\,\Delta\phi_{N-1}[k]+\{1-f'_1(\phi_{N-2}{}^*)\}\,\Delta\phi_{N-2}[k]$$
$$\Delta\phi_{N-2}[k+1]=\{f'_1(\phi_{N-1}{}^*)-1\}\,\Delta\phi_{N-1}[k]+\{1-f'_1(\phi_{N-3}{}^*)\}\,\Delta\phi_{N-3}[k] \quad (67)$$

$$\Delta\phi_3[k+1]=\{f'_1(\phi_{N-1}{}^*)-1\}\,\Delta\phi_{N-1}[k]+\{1-f'_1(\phi_2{}^*)\}\,\Delta\phi_2[k]$$
$$\Delta\phi_2[k+1]=\{f'_1(\phi_{N-1}{}^*)-1\}\,\Delta\phi_{N-1}[k]+\{1-f'_1(\phi_1{}^*)\}\,\Delta\phi_1[k]$$
$$\Delta\phi_1[k+1]=\{f'_1(\phi_{N-1}{}^*)-1\}\,\Delta\phi_{N-1}[k].$$

These equations can be written as a single matrix equation as follows: $\Delta[k+1] = S\,\Delta[k]$ where $\Delta[k] = [\Delta\phi_{N-1}[k], \Delta\phi_{N-2}[k], \ldots, \Delta\phi_2[k], \Delta\phi_1[k]]^T$ and S is the following N−1 dimensional matrix:

$$\begin{pmatrix} f_1'(\phi_{N-1}^*)-1 & 1-f_1'(\phi_{N-2}^*) & 0 & \cdots & 0 \\ f_1'(\phi_{N-1}^*)-1 & 0 & 1-f_1'(\phi_{N-3}^*) & \cdots & 0 \\ \vdots & \vdots & \vdots & \cdots & \vdots \\ \vdots & \vdots & \vdots & \cdots & 1-f_1'(\phi_1^*) \\ f_1'(\phi_{N-1}^*)-1 & 0 & 0 & \cdots & 0 \end{pmatrix}$$

The eigenvalues of the above matrix determine the stability of the splay mode. The mode is predicted to be stable only if the absolute value of all eigenvalues is less than 1.

Existence of the symmetric splay modes in which the firing intervals between successive firing of neurons in the circuit were equal can be determined as follows (see Fig. 12B). The first stimulus interval in each cycle can be written in terms of a single phase. The stimulus intervals for i from 2 to (N−1) can be calculated by adding the first order resetting due to the input that marks the start of the interval to the difference between the phases at which the inputs bounding the interval are received. The stimulus interval, $ts_N[\infty]$ is the recovery interval due to the last input in the cycle. Thus, $ts_1[\infty] = P_i\{\phi_1{}^*\}$, $ts_i[\infty] = P_i\{\phi_i{}^* - \phi_{i-1}{}^* + f_1(\phi_{i-1}{}^*)\}$ for i=2…(N−1) and $ts_N[\infty] = P_i\{1 - \phi_{N-1}{}^* + f_1(\phi_{N-1}{}^*)\}$. An iterative method to find the fixed points corresponding to a splay mode can then be employed. $\phi^*{}_{N-1}$ is sampled between 0 and 1 to determine the values that produce the same value of $ts_N[\infty]$ whether it is calculated directly from the expression for $ts_N[\infty]$ or iteratively from the expression for $ts_i[\infty]$ starting from the value of $\phi^*{}_1$ that produces the same value of $ts_N[\infty]$ as the direct method.

For a rotationally symmetric system in which each neuron receives exactly the same input, we obtain the single matrix shown above. If not, then the matrices corresponding to each firing time until the pattern repeats (N matrices) must be multiplied in the correct order. The resulting system on linearization about a presumed fixed point turns out to be such that:

$$\Delta\phi[k+N]=M_N M_{N-1}\cdots M_2 M_1\,\Delta\phi[k] \quad (68)$$

where $\Delta\phi[k]$ is the vector containing the perturbations from the fixed point representing a steady phase locked firing pattern as in Fig. 12B. The index k corresponds to the k^{th} spike. Each matrix M_m is given below and maps the phases from one spike time to the next;

$$\begin{pmatrix} \alpha\left(\frac{P_{m+1}}{P_{m+2}}\right) & \left(1-f'_{1,m+2}\left(\phi^*_{m+2,N-2}\right)\right) & 0 & \dots & 0 \\ \alpha\left(\frac{P_{m+1}}{P_{m+3}}\right) & 0 & \left(1-f'_{1,m+3}\left(\phi^*_{m+3,N-3}\right)\right) & \dots & 0 \\ \vdots & \vdots & \vdots & \dots & \vdots \\ \alpha\left(\frac{P_{m+1}}{P_{m+N-1}}\right) & \vdots & \vdots & \dots & \left(1-f'_{1,m+N-1}\left(\phi^*_{m+N-1,1}\right)\right) \\ \alpha\left(\frac{P_{m+1}}{P_{m+N}}\right) & 0 & 0 & \dots & 0 \end{pmatrix}$$

where $\alpha = \{f_{1,m+1}'(\phi^*_{m+1,N-1}) - 1\}$ and $(f_{1i}'(\phi_{ik}^*))$ represents the slope of the first order PRC at the locking point of the k^{th} input to the i^{th} neuron. Here, addition is modulo N and P_i indicates the intrinsic period of the i^{th} neuron. The matrix $M(=M_N M_{N-1} \cdots M_2 M_1)$ will still have (N−1) eigenvalues and will determine of the splay mode. This result was alluded to but not explicitly derived in Achuthan and Canavier ([17]).

III.4.3 Cluster modes

III.4.3.1 Two 1:1 locked reciprocally coupled populations: The applicability of PRC theory under the pulsatile coupling assumption can be greatly extended if we can apply it to populations of neurons rather than just single neurons. Figure 10A illustrates the concept of treating a population of synchronous oscillators as a single oscillator that has a stronger effect on its targets than a single oscillator since all component oscillators discharge at once. The simplification is derived from assuming the population has a PRC similar to that of an individual oscillator ([13], [17], and [28]). An early approach was to consider synchronous interactions within a cluster ((64) applied to each cluster in isolation) separately from the alternating firing pattern that characterizes between cluster interactions ((68) for several clusters, or (20) for the case of just two clusters). Treating between and within cluster interactions separately does not always produce correct stability results ([17]). Therefore, a novel generic proof for determining the stability of two populations of arbitrary size has been developed ([30] and [31]) which shows how the between cluster interactions can stabilize clusters that cannot synchronize in isolation. In essence, the within cluster eigenvalue obtained by evaluating (64) at zero and one is scaled by $1-f_1(\phi^*)$, where ϕ^* is the phase at which input from the other cluster is received. The main idea for the proof was to consider perturbation of a single neuron within one cluster only, keeping the rest of the cluster configuration intact (see Fig. 10B). A rigorous proof for cluster modes when there are more than two clusters is an open question, but the two cluster case is most likely to be physiologically significant as it is difficult to find solutions with more than two clusters ([17] and [63]).

III.4.3.2 Two N:1 locked reciprocally coupled populations: Canavier et al. ([28]) studied N:1 phase locking between two populations of Wang and Buzsaki ([14]) model neurons connected via inhibitory synapses within a population and excitatory synapses between populations. The connections were all to all but with two distinct types of synapses intended to approximate local cortical connections via inhibitory interneurons and distal connections via excitatory pyramidal cells, with conduction delays ignored. As in [17] each cluster was treated as a single oscillator with a conductance strength scaled by the number of simultaneously active synapses (see Fig. 10A). Equation (19) was used to predict within cluster synchronization since each cluster was comprised of only two neurons, and the methods in II.2.6 were successfully used to predict 2:1 locking between clusters.

IV. Summary and Significance

IV.1 Summary

The rhythmic activity of the cardiac pacemaker cells, pancreatic cells; neural circuits that underlie central pattern generators (CPGs) that form the basis of breathing and locomotion in invertebrates as well as vertebrates; rhythmic activity of the circadian cells from the suprachiasmatic nucleus and the flashings of fireflies are some of the well known biological examples of pulse coupled oscillators ([1–4], [34–38]). In this article we have reviewed the use of phase resetting theory to study the firing activity of pulse coupled neural oscillators ([2–4], [7], [17], [20], [24–26], [28], [39–41]). PRCs have been used to predict the rhythmic activity of networks of pulse coupled neurons using the NPFO based map approach as well as by PFO maps. In the former no assumption regarding the firing order of the neurons is required whereas in the latter existence and stability criteria for a variety of firing patterns is based on the assumption that the firing order is predetermined. The NPFO map may produce different firing patterns depending upon how it is initialized because no fixed, predetermined firing order is assumed.

IV. 2 Potential Applications

Global synchronization is relevant to a number of important biological problems such as cognitive functions exhibited by transiently synchronized assemblies of neurons ([37]); synchronization between distant human brain regions for word recollection ([42]) and whether an image is recognized as a face ([43]). Pathological synchrony could lead to epileptic seizures ([44] and [45]) and tremor ([46]), and there is consistent evidence for a reduction of synchronization in schizophrenia ([47]). Neural circuits that underlie CPGs produce a repetitive pattern of motor activity ([48]), such as locomotion or respiration, even in the absence of sensory feedback or patterned input from higher brain centers. An influential theory ([38], [49]) suggests that cortical rhythms and circuits evolved from motor rhythms and circuits, and are therefore likely to share basic principles of organization and dynamic function. In addition, pathological rhythms such as absence epileptic seizures have been postulated to arise from phase locking between thalamic and cortical sites ([50]).

Since PRCs can be measured for biological neurons, the methods presented in this review can provide insight into the synchronization tendencies of neural networks. The motivation for the type of work described in this review was clearly articulated by Netoff et al. ([54]). We would like to understand synchronization phenomena that depend upon the "interactions of many neurons with distinct cellular populations and patterns of connectivity in different sub-regions", but our ability to record from many single neurons simultaneously is limited. Instead, we can attempt to characterize the dynamics of network components and then construct network models that make predictions regarding synchronization tendencies, some of which can be tested using dynamic clamp techniques ([59], [60]).

IV.3 Dynamic Clamp as a tool for studying pulse coupling

The dynamic clamp technique [70],[71]) uses a computer to inject artificial membrane or synaptic conductances in biological neurons. The membrane potential of the biological neuron is continuously measured and used in a mathematical model to compute the current that would result from the virtual conductance at each time step, and this current is injected into the biological neuron ([69]). Some interesting applications of the dynamic clamp technique that are relevant to the study of pulse coupled oscillators are 1) to inject virtual synaptic conductances in order to measure PRCs, 2) to construct hybrid circuits in which artificial synapses couple a biological neuron to other biological or model neurons, and 3) to inject ionic currents to determine their effect on the PRC. Hybrid circuits ([13], [18], [24],

[54], [72]) have been used to test the predictions based on the PRCs measured in response to the injection of virtual synaptic conductances.

In hybrid neuronal networks ([13], [18], [24], [54], [72]), the dynamic clamp computer continuously solves the differential equations that describe the synapses as well as any model neuron(s) that are connected to the biological neuron (s). The existence and stability criteria for 1:1 phase locking between two non-identical pulse coupled oscillators were successfully tested in a hybrid network of one bursting model neuron and one physiological bursting neuron ([24]) with reciprocal inhibition. Similar hybrid neuronal networks with excitatory synapses were shown not to promote phase-locking in central pattern generating networks as reliably as with inhibitory synapses ([18]). Netoff et al. ([72]) constructed reciprocally excitatory, reciprocally inhibitory, and heterogeneous (excitatory-inhibitory) two neuron hybrid networks comprised of either two biological neurons or one model neuron and one spiking neuron using entorhinal stellate cells and/or OLM (Oriens-Lacunosum-Moleculare) interneurons (and their model counterparts), and successfully predicted their activity using the STRC (see section III.2.1).

Pervouchine et al. ([13]) extended the work of Netoff et al. ([72]) to examine the contribution of a specific conductance (the hyperpolarization activated cation conductance) to the PRC and hence to synchronization in similar hybrid networks. They demonstrated that augmenting this conductance increased the magnitude of the advances observed at early phases and this in turn increased the tendency of the neurons to synchronize at theta frequencies when coupled. The activation of this current would therefore promote theta power, which is important in memory encoding ([81]).

IV. 4 Caveats regarding PRC based methods for pulse coupled networks

Pulsatile coupling methods have been applied to a number of circuit architectures in order to derive stability results for phase locked modes; in the most general cases, the stability depends only on the slope of the resetting curves at the locking points in a firing pattern that repeats every network cycle. Firing orders that are not constant from cycle to cycle were considered by Maran and Canavier ([15]) as well as Oh and Matveev ([16]). In these papers, the leading neuron can switch from cycle to cycle, but the firing order over a two-cycle interval was still fixed. Stability in the case of changing firing order is an open problem because the PFO maps only work with a particular assumed firing order (but see Timme et al. ([57], [58]). In general, pulsatile coupling methods can be extended to inputs that are not strictly pulsatile under the assumption that the effect of a perturbation has dissipated by the time the next one is received. This implies that only first and second order PRCs can be accommodated, which is limitation of the method; the second order resetting from the previous cycle must be complete by the time the first stimulus in each cycle is received. The likelihood of a violation of this assumption is much greater in networks comprised of oscillators that receive multiple inputs per cycle compared to those that receive only a single input per cycle. The violation of the assumption of a constant firing order is also problematic. Slow currents that cause adaptation from cycle to cycle also violate the assumption of pulsatile coupling. One possible solution to the problem of higher order components of the resetting is to apply repetitive inputs at a fixed delay rather than just a single pulse ([52]), and another solution utilized an empirically derived renormalization factor to account for second order effects that continued beyond the first stimulus interval in a cycle, and even for third order resetting ([61], [62]).

IV.5 Comparison of Different Approaches

One early approach ([3], [4], [5], [6]) relied upon assuming a monotonically increasing concave down function for the evolution of the component oscillators, such as would be

observed for a leaky integrate and fire oscillator, and to further assume that the coupling increments (or decrements) this function by a fixed amount, which implicitly defines a PRC. The results obtained by this approach are a special case of the more general PRC based methods also described here, as they can be rederived by simply using this implicit PRC in the more general existence and stability criteria for arbitrary PRCs. Thus proofs that make fewer assumptions about the nature of the phase resetting are more generally applicable, since PRCs of many different shapes can be observed both in model and biological neurons, not just the implicit shape assumed by Mirollo and Strogatz and others. Another improvement difference over earlier methods is the inclusion of second-order resetting, which often needs to be considered in evaluating the stability of synchrony, because perturbations from synchrony include inputs received just prior to a spike, when second order effects are maximal.

Whereas here we have simplified the analysis by assuming that the coupling is pulsatile, an alternate way to simplify the analysis is to assume that the coupling is so weak that the network period and the periods of the component oscillators are sufficiently similar that the phases of the oscillator can be used directly without converting the phases back to time intervals using the different periods for comparison in the time domain. This approach assumes that phase resetting is proportional to the amplitude of the perturbation and that the phase resetting due to coupling can be obtained by summing the resetting at each phase in the cycle without updating the phase for resetting that occurs earlier in the cycle. Finally, the relative phases are assumed to change very slowly. This last assumption is violated by patterns such as synchronization that are established quickly, within one or a few cycles. The results obtained by this method are independent of the strength of the coupling, and therefore cannot predict how stability changes as the conductance strength changes (see Fig. 2). Furthermore, they cannot distinguish between first and second order resetting, and the stability results neglect terms that are products of the PRC slopes in different oscillators ([11]). On the other hand, they have been extensively used ([82], [83]) and do not have the limitation, as pulse-coupled methods do, that the effect of one input must die out before the next is received. The application of phase resetting methods to systems in which the coupling is neither weak nor pulsatile is very much an open problem ([64]).

Acknowledgments

This work was supported by NIH NS54281 under the CRCNS program and MH 85387 to CCC.

REFERENCES

1. Kuramoto, Y. Chemical oscillations, waves and turbulence. Berlin: Springer-Verlag; 1984.
2. Winfree, AT. The geometry of biological time. New York: Springer-Verlag; 2001.
3. Mirollo RE, Strogatz SH. Synchronization of pulse coupled biological oscillators. SIAM J. Appl. Math 1990;50:1645–1662.
4. Peskin, CS. Mathematical Aspects of Heart Physiology, Courant Institute of Mathematical Sciences. New York: New York University; 1975. p. 268-278.
5. Ernst U, Pawelzik K, Geisel T. Synchronization induced by temporal delays in pulse coupled oscillators. Phys. Rev. Lett 1995;74:1570–1573. [PubMed: 10059062]
6. Ernst U, Pawelzik K, Geisel T. Delay-induced multistable synchronization of biological oscillators. Phys. Rev. E 1998;57:2150–2162.
7. Canavier CC, Butera RJ, Dror RO, Baxter DA, Clark JW, Byrne JH. Phase response characteristics of model neurons determine which patterns are expressed in a ring circuit model of gait generation. Biol. Cyber 1997;77:367–380.
8. Canavier CC, Baxter DA, Clark JW, Byrne JH. Control of multistability in ring circuits of oscillators. Biol. Cyber 1999;80:87–102.

9. Canavier, CC.; Baxter, DA.; Byrne, JH. Encyclopedia of Life Sciences. Vol. 16. London: Nature Publishing Group; 2002. Repetitive firing of action potentials: a dynamic analysis; p. 271-282.
10. Luo C, Clark JW, Canavier CC, Baxter DA, Byrne JH. Multimodal behavior in a four neuron ring circuit: mode switching. IEEE Trans. Biomed. Eng 2004;51:205–218. [PubMed: 14765693]
11. Achuthan, S.; Canavier, CC. Intrinsic and synaptic dynamics have separate effects on phase locking for weakly coupled oscillators. Conference Abstract: 2010 South East Nerve Net (SENN) and Georgia/South Carolina Neuroscience Consortium (GASCNC) conferences; doi: 10.3389/conf.fnins.2010.04.00001
12. Acker CD, Kopell N, White JA. Synchronization of strongly coupled excitatory neurons: relating network behavior to biophysics. J. Comp. Neurosci 2003;15:71–90.
13. Pervouchine DD, Netoff TI, Rostein HG, White JA, Cunningham MO, Whittington MA, Kopell NJ. Low dimensional maps encoding dynamics in entorhinal cortex and hippocampus. Neural Comput 2006;18:2617–2650. [PubMed: 16999573]
14. Wang XJ, Buzsaki G. Gamma oscillation by synaptic inhibition in a hippocampal interneuronal network model. J. Neurosci 1996;16:6402–6413. [PubMed: 8815919]
15. Maran SK, Canavier CC. Using phase resetting to predict 1:1 and 2:2 locking in two neuron networks in which firing order is not always preserved. J. Comput. Neurosci 2008;24:37–55. [PubMed: 17577651]
16. Oh M, Matveev V. Loss of phase-locking in non-weakly coupled inhibitory networks of type-I model neurons. J. Comput. Neurosci 2009;26:303–320. [PubMed: 18690530]
17. Achuthan S, Canavier CC. Phase resetting curves determine synchronization, phase-locking, and clustering in networks of neural oscillators. J. Neurosci 2009;29:5218–5233. [PubMed: 19386918]
18. Sieling FH, Canavier CC, Prinz AA. Predictions of phase-locking in excitatory hybrid networks: Excitation does not promote phase-locking in pattern generating networks as reliably as inhibition. J. Neurophysiol 2009;102:69–84. [PubMed: 19357337]
19. Oprisan SA, Canavier CC. Stability analysis of entrainment by two periodic inputs with a fixed delay. Neurocomputing 2003;52–54:59–63.
20. Perkel DH, Schulman JH, Bullock TH, Moore GP, Segundo JP. Pacemaker neurons: effects of regularly spaced synaptic input. Science 1964;145:61–63. [PubMed: 14162696]
21. Canavier, CC.; Achuthan, S. History of the application of phase resetting curves to neurons coupled in a pulsatile manner. In: Schultheiss, NW.; Prinz, AA.; Butera, RJ., editors. Phase response curves in Neuroscience. Springer; 2009. submitted
22. Foss J, Milton J. Multistability in recurrent neural loops arising from delay. J. Neurophysiol 2000;84:975–985. [PubMed: 10938321]
23. Dror RO, Canavier CC, Butera RJ, Clark JW, ByrnE JH. A mathematical criterion based on phase response curves for stability in a ring of coupled oscillators. Biol.Cybern 1999;80:11–23. [PubMed: 20809292]
24. Oprisan SA, Prinz AA, Canavier CC. Phase resetting and phase locking in hybrid circuits of one model and one biological neuron. Biophys. J 2004;87:2283–2298. [PubMed: 15454430]
25. Oprisan SA, Canavier CC. Stability analysis of rings of pulse-coupled oscillators: the effect of phase resetting in the second cycle after the pulse is important at synchrony and for long pulses. Differential Equations and Dynamical Systems 2001;9:242–259.
26. Goel P, Ermentrout GB. Synchrony, stability, and firing patterns in pulse coupled oscillators. Physica D 2002;163:191–216.
27. Woodman M, Canavier CC. Phase locking of pulse coupled oscillators with delays is determined by the phase response curve, Frontiers in Systems Neuroscience. Computational and systems neuroscience. 2009 doi:10.3389/conf.neuro.06.2009.03.139.
28. Canavier CC, Gurel Kazanci F, Prinz AA. Phase resetting curves allow for simple and accurate prediction of robust N:1 phase locking for strongly coupled neural oscillators. Biophys. J 2009;97:59–73. [PubMed: 19580744]
29. Morris C, Lecar H. Voltage oscillations in the barnacle giant muscle fiber. Biophys. J 1981;35:193–213. [PubMed: 7260316]
30. Chandrasekaran L, Achuthan S, Canavier CC. Stability of two clustered solutions in networks of neuronal oscillators using phase resetting curves. submitted to Phys. Rev. E. 2009

31. Achuthan, S.; Chandrasekaran, L.; Canavier, CC. Phase resetting curve analysis of global synchrony, the splay mode and clustering in N neuron all to all pulse coupled networks. In: Schultheiss, NW.; Prinz, A.; Butera, R., editors. Phase resetting curves in neuroscience. Springer; 2009. submitted
32. Dror RO, Canavier CC, Butera RJ, Clark JW, Byrne JH. A mathematical criterion based on phase response curves for stability in a ring of coupled oscillators. Biol.Cybern 1999;80:11–23. [PubMed: 20809292]
33. Achuthan, S.; Sieling, FH.; Prinz, AA.; Canavier, CC. Phase resetting curves in presence of heterogeneity and noise. In: Ding, M.; Glanzman, D., editors. Neuronal variability and its functional significance. Oxford University Press; 2009. in press
34. Winfree AT. Biological rhythms and the behavior of populations of coupled oscillators. J. Theor. Biol 1967;16:15–42. [PubMed: 6035757]
35. Buck J. Synchronous rhythmic flashing of fireflies II. Quart. Rev. Biol 1988;63:265–289. [PubMed: 3059390]
36. de la Iglesia HO, Cambras T, Schwartz WJ, Diez-Noguera A. Forced desynchronization of dual circadian oscillators within the rat suprachiasmatic nucleus. Curr. Biol 2004;14:796–800. [PubMed: 15120072]
37. Buzsaki, G. Rhythms of the brain. New York: Oxford University Press Inc.; 2006.
38. Yuste R, MacLean JN, Smith J, Lansner A. The cortex as a central pattern generator. Nature Rev. Neurosci 2005;6:477–483. [PubMed: 15928717]
39. Glass, L.; Mackey, MC. From clocks to chaos: the rhythms of life. Princeton, N.J.: Princeton University Press; 1988.
40. Strogatz, SH. Sync: how order emerges from chaos in the universe, nature, and daily life. New York: Hyperion; 2003.
41. Pikovsky, A.; Rosenblum, M.; Kurths, J. Synchronization: a universal concept in nonlinear sciences. Cambridge, U. K: Cambridge University Press; 2001.
42. Fell J, Klaver P, Lehnertz K, Grunwald T, Schaller C, Elger CE, Fernandez G. Human memory formation is accompanied by rhinal-hippocampal coupling and decoupling. Nat. Neurosci 2001;4:1259–1264. [PubMed: 11694886]
43. Rodriguez E, George N, Lachaux JP, Martinerie J, Renault B, Varela FJ. Perception's shadow: long distance synchronization of human brain activity. Nature 1999;397:430–433. [PubMed: 9989408]
44. Huguenard JR, McCormick DA. Thalamic synchrony and dynamic regulation of global forebrain oscillations. Trends Neurosci 2007;30:350–356. [PubMed: 17544519]
45. Traub RD, Jefferys JG. Are there unifying principles underlying the generation of epileptic afterdischarges in vitro? Prog. Brain Res 1994;102:383–394. [PubMed: 7800828]
46. Hammond C, Bergman H, Brown P. Pathological synchronization in Parkinson's disease: networks, models and treatments. Trends Neurosci 2007;30:357–364. [PubMed: 17532060]
47. Uhlhaas PJ, Singer W. Neural synchrony in brain disorders: relevance for cognitive dysfunctions and pathophysiology. Neuron 2006;52:155–168. [PubMed: 17015233]
48. Stein, SG.; Grillner, S.; Selverston, AI.; Stuart, DG., editors. Neurons, networks, and motor behavior. Cambridge, MA: MIT Press; 1997.
49. Llinas, RR. I of the Vortex: From neurons to self. Cambridge, MA: MIT Press; 2002.
50. Velazquez JLP, Galan RF, Dominguez LG, Leshchenko Y, Lo S, Belkas J, Erra RG. Phase response curves in the characterization of epileptiform activity. Phys. Rev. E 2007;76:061912.
51. Mancilla JG, Lewis TJ, Pinto DJ, Rinzel J, Connors BW. Synchronization of electrically coupled pairs of inhibitory interneurons in neocortex. J. Neurosci 2007;27:2058–2073. [PubMed: 17314301]
52. Cui J, Canavier CC, Butera RJ. Functional phase response curves: a method for understanding synchronization of adapting neurons. J. Neurophysiol 2009;102:387–398. [PubMed: 19420126]
53. Rubin, JE.; Terman, D. Geometric singular perturbation analysis of neuronal dynamics. In: Fiedler, B., editor. Handbook of dynamical systems: toward applications. Vol. vol. 2. Amsterdam: Elsevier; 2002.

54. Netoff TI, Banks MI, Dorval AD, Acker CD, Haas JS, Kopell NK, White JA. Synchronization in hybrid neuronal networks of the hippocampal formation. J. Neurophysiol 2005;93:1197–1208. [PubMed: 15525802]
55. Rinzel, J.; Ermentrout, GB. Analysis of neural excitability and oscillations. In: Koch, C.; Segev, I., editors. Methods in neuronal modeling from ions to networks. Cambridge, MA: MIT Press; 1998.
56. Senn W, Urbanczik R. Similar nonleaky integrate and fire neurons with instantaneous couplings always synchronize. SIAM J. Appl. Math 2000;61:1143–1155.
57. Timme M, Wolf F, Geisel T. Coexistence of regular and irregular dynamics in complex networks of pulse coupled oscillators. Phys. Rev. Lett 2002;89:258701. [PubMed: 12484926]
58. Timme M, Wolf F. The simplest problem in the collective dynamics of neural networks: is synchrony stable ? Nonlinearity 2008;21:1579.
59. Sharp AA, O'Neil MB, Abbott LF, Marder E. The dynamic clamp: artificial conductances in biological neurons. Trends Neurosci 1993a;16:389–394. [PubMed: 7504352]
60. Sharp AA, O'Neil MB, Abbott LF, Marder E. Dynamic clamp: computer-generated conductances in real neurons. J. Neurophysiol 1993b;69:992–995. [PubMed: 8463821]
61. Talathi SS, Hwang DU, Miliotis A, Carney PR, Ditto W. Predicting synchrony in a heterogeneous pulse coupled oscillators. Phys. Rev. E 2009;80:021908.
62. Talathi SS, Hwang DU, Carney PR, Ditto W. Synchrony with shunting inhibition in feed-forward inhibitory networks. submitted J. Comp. Neurosci.
63. Golomb D, Wang XJ, Rinzel J. Synchronization properties of spindle oscillations in a thalamic reticular nuclues model. J. Neurophysiol 1994;72:1109–1126. [PubMed: 7807198]
64. Ermentrout GB, Chow CC. Modeling neural oscillations. Physiol. Behav 2002;77:629–633. [PubMed: 12527010]
65. Gerstner W. Rapid phase locking in systems of pulse coupled oscillators with delays. Phys. Rev. Lett 1996;76:1755–1758. [PubMed: 10060509]
66. Izhikevich, EM. Dynamical systems in neuroscience: the geometry of excitability and bursting. Cambridge, MA: The MIT Press; 2007.
67. Foss, J. Ph.D. thesis. Chicago, IL: The University of Chicago; 1999. Control of multistability in neural feedback systems with delay.
68. Pavlidis, T. Biological oscillators: their mathematical analysis. New York, NY: Academic Press; 1973.
69. Prinz AA. The dynamic clamp a decade after its invention. AxoBits 2004;40:6–7.
70. Prinz AA, Abbott LF, Marder E. The dynamic clamp comes of age. Trends Neurosci 2004;27:218–224. [PubMed: 15046881]
71. Destexhe, A.; Bal, T. New York, NY: Springer; 2009. Dynamic-clamp: from principles to applications, al systems in neuroscience: the geometry of excitability and bursting.
72. Netoff TI, Acker CD, Bettencourt JC, White JA. Beyond two-cell networks: experimental measurement of neuronal responses to multiple synaptic inputs. J. Comput Neurosci 2005;18:287–295. [PubMed: 15830165]
73. Ermentrout, GB.; Beverlin, B., II; Netoff, T. Phase response curves to measure ion channel effects on neurons. In: Schultheiss, NW.; Prinz, AA.; Butera, RJ., editors. Phase response curves in Neuroscience. Springer; 2009. submitted
74. Gutkin BS, Ermentrout GB, Reyes AD. Phase-response curves give the responses of neurons to transient inputs. J. Neurophysiol 2005;94:1623–1635. [PubMed: 15829595]
75. Hodgkin AL. The local electric changes associated with repetitive action in a non medullated axon. J. Physiol 1948;107:165–181. [PubMed: 16991796]
76. Ermentrout GB, Pascal M, Gutkin BS. The effects of spike frequency adaptation and negative feedback on the synchronization of neural oscillators. Neural Comput 2001;13:1285–1310. [PubMed: 11387047]
77. Hauptmann C, Roulet JC, Niederhauser JJ, et al. External trial deep brain stimulation device for the application of desynchronizing stimulation techniques. J. Neural. Eng 2009;6:066003. [PubMed: 19837998]

78. Osorio I, Frei MG. Seizure abatement with single dc pulses: is phase resetting at play ? Intl. J. Neural Syst 2009;3:149–156.
79. Rizzuto DS, Madsen JR, Broomfield EB, et al. Reset of human neocortical oscillations during a working memory task. Proc. Natl. Acad. Sci 2003;100:7931–7936. [PubMed: 12792019]
80. Llinás RR. Inferior olive oscillation as the temporal basis for motricity and oscillatory reset as the basis for motor error correction. Neurosci 2009;162:797–804.
81. Rutishauser U, Ross IB, Mamelak AM, Schuman EM. Human memory strength is predicted by theta-frequency phase-locking of single neurons. Nature 2010;464:903–907. [PubMed: 20336071]
82. Ermentrout GB, Kopell N. Oscillator death in systems of coupled neural oscillators. SIAM J. Appl. Math 1990;50:125–146.
83. Ermentrout GB, Kopell N. Multiple pulse interactions and averaging in coupled neural oscillators. J. Math Biol 1991;29:195–217.
84. Pfeuty B, Mato G, Golomb D, Hansel D. Electrical synapses and synchrony ; the role of intrinsic currents. J. Neurosci 2003;23:6280–6294. [PubMed: 12867513]

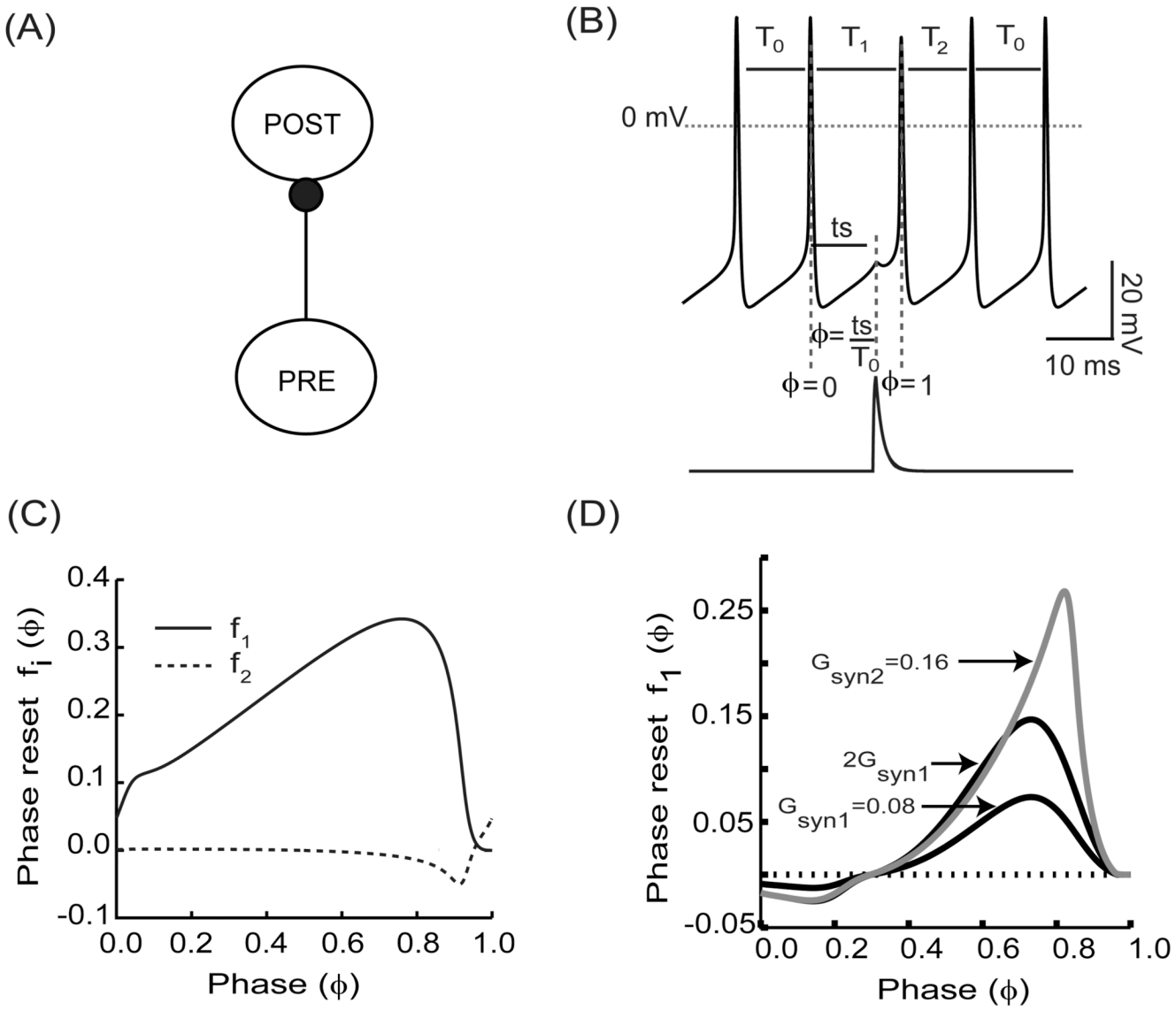

FIGURE 1.

Phase Resetting Curve. (A) Open loop configuration. PRE stands for the pre-synaptic neuron and POST stands for the post-synaptic neuron (B) The voltage waveform represents a regular spiking neuron with intrinsic period T_0. The lower trace corresponds to the post-synaptic conductance resulting from a spike in a pre-synaptic neuron. The normalized change in cycle period length as a result of the perturbation received at a phase $\phi = ts/T_0$ is the phase resetting. T_1 represents the period of the cycle in which the stimulus is received. The following cycle period is represented by T_2. (C) Example of first order ($f_1(\phi)$, solid line) and second order ($f_2(\phi)$, dashed line) phase resetting curves. (D) PRCs are nonlinear with respect to conductance strengths. PRCs corresponding to g_{syn1} (black color) and g_{syn2} (gray color). For strong coupling, the resetting does not add linearly as evidenced by the changing shape as the conductance strength is increased to represent a single input (g_{syn1}), two simultaneous inputs (g_{syn2}). Note that $g_{syn2} \neq 2g_{syn1}$ (black color).

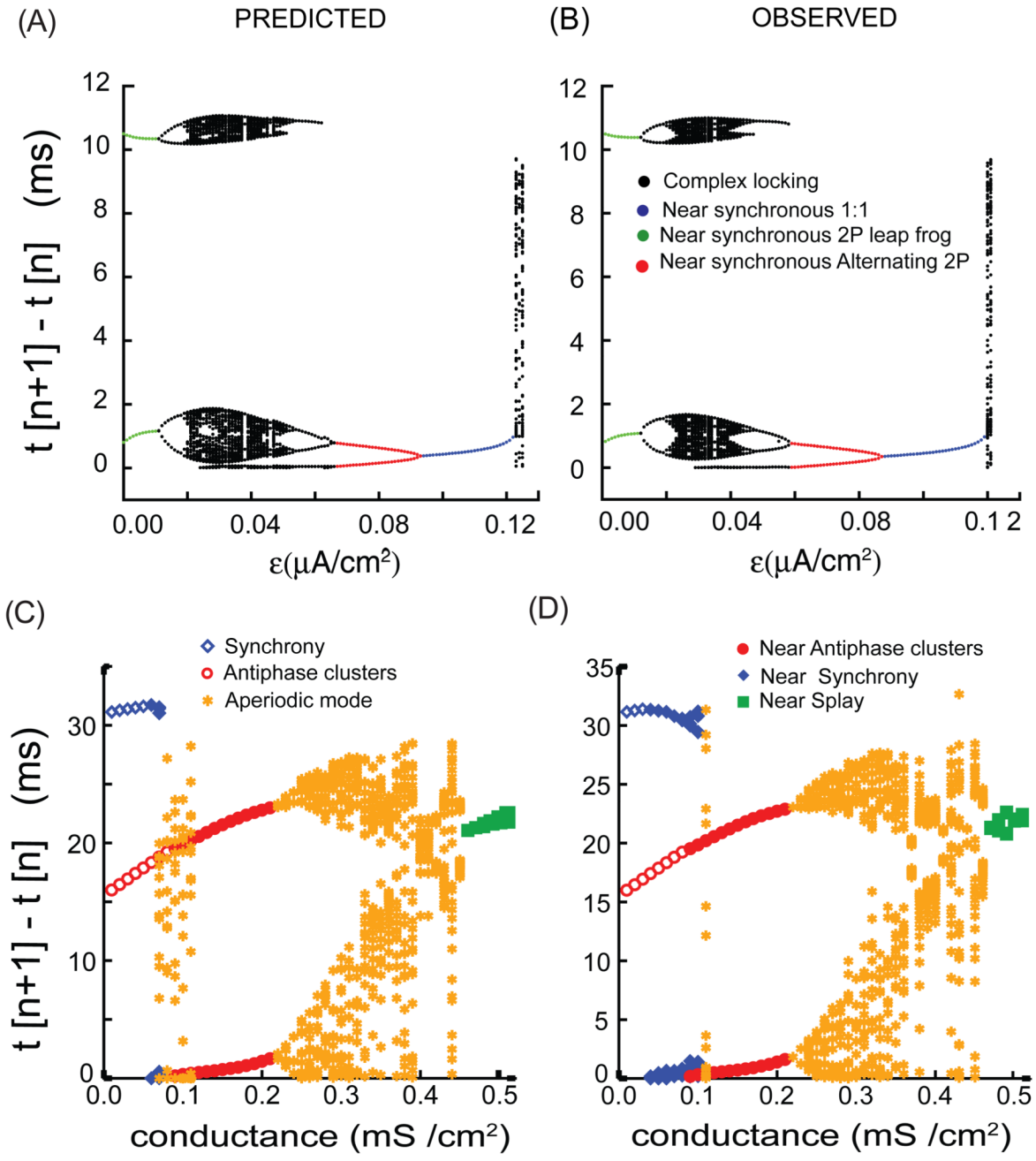

FIGURE 2.

Complex modes observed in a two neuron and a four neuron network are predicted quite well by the NPFO maps. These results are for network with type I excitability and inhibitory synaptic connectivity. As a function of the heterogeneity parameter, ε ([15]), for a two neuron network of Wang and Buzsaki model neurons: (A) predicted firing intervals for the various modes from the NPFO map and (B) Observed firing intervals produced by integrating the full system of differential equations. Similarly, as a function of the synaptic conductance strength in the four neuron network of Wang and Buzsaki model neurons ([17]): (A) the firing intervals produced by the NPFO map and (B) firing intervals produced by integrating the full system of differential equations. The modes labeled antiphase clusters

or near antiphase clusters refer to two clusters in antiphase or near antiphase, whereas the synchronous and nearly synchronous modes refer to a single cluster.

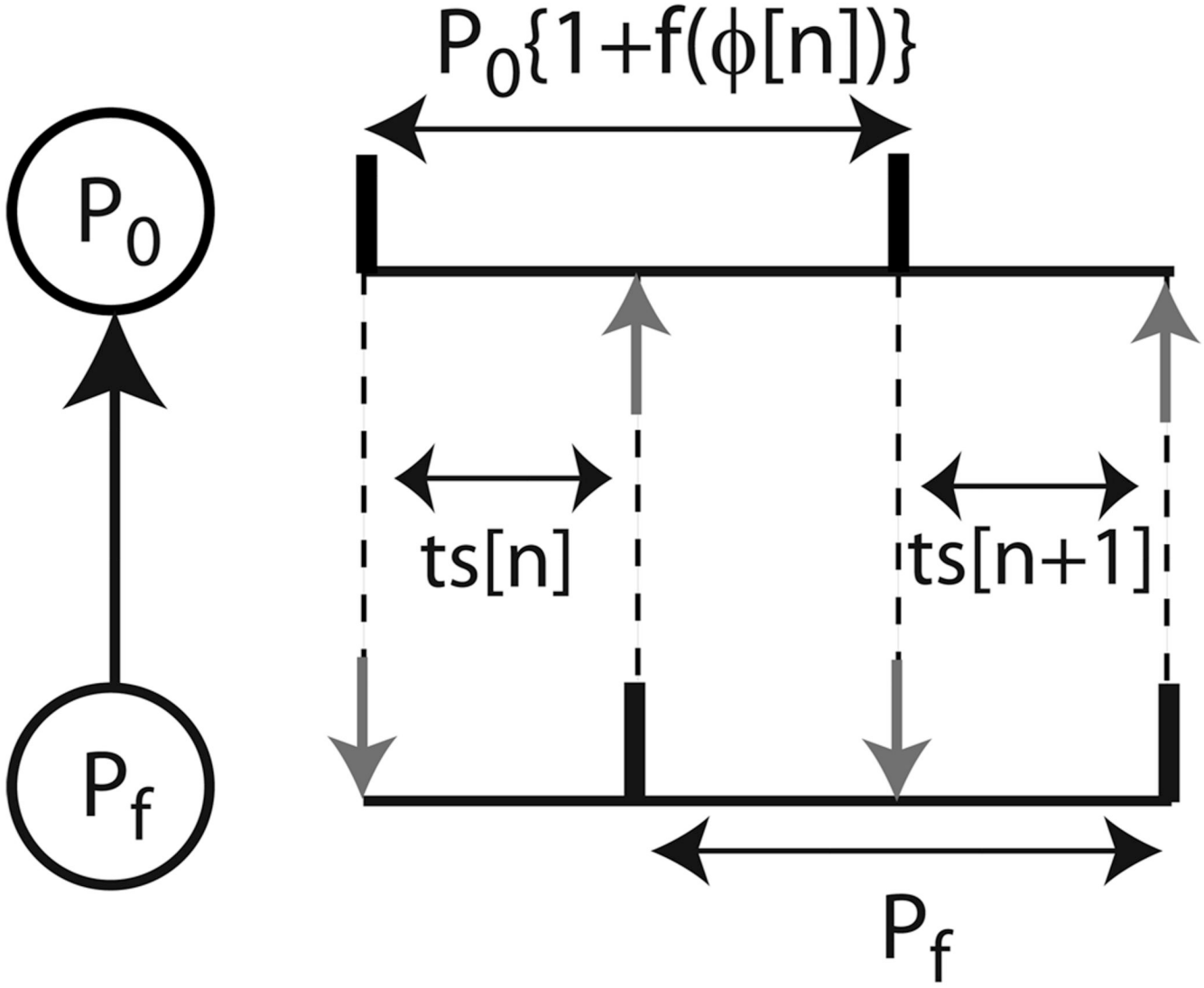

FIGURE 3.

A periodically forced oscillator. Stimulus intervals (ts) in the n^{th} and $(n+1)^{st}$ cycles in a phase locked mode with no delays is shown here. The black vertical bars indicate firing times and the vertical gray arrows indicate neuronal inputs arriving at a phase ϕ (= ts / P_0). P_0 represents the period of the forced oscillator and P_f represents the period of the forcing oscillator.

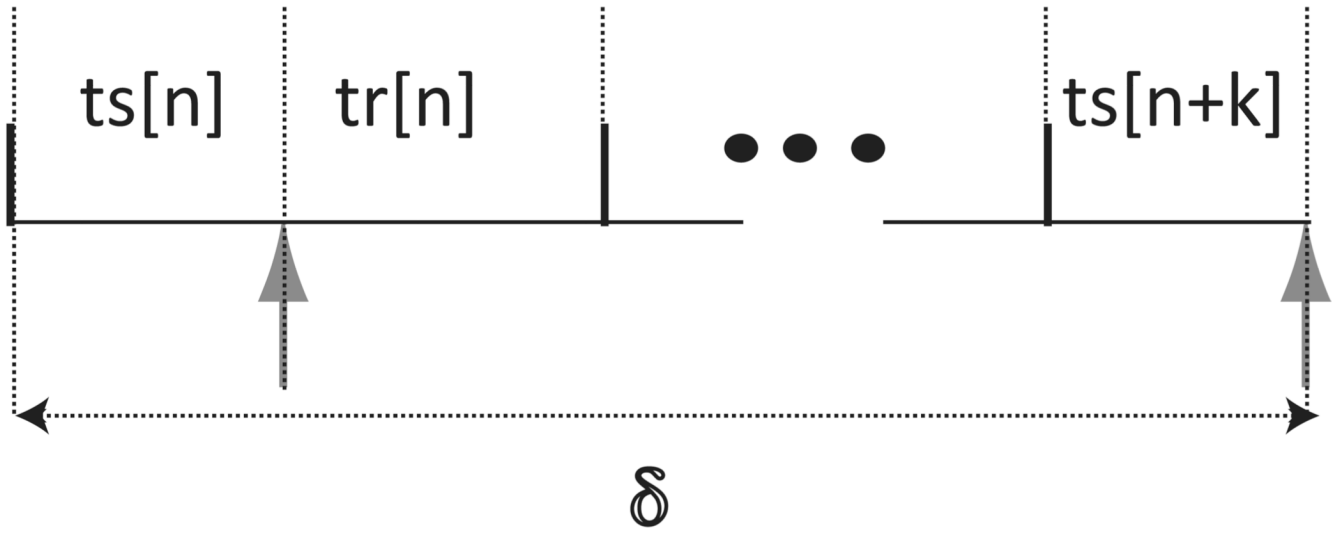

FIGURE 4.
Neural firing time map with delays of arbitrary lengths for a forced oscillator with a feedback input that has a fixed delay (δ) from each time the oscillator fires. Stimulus intervals (ts_i) denote the time elapsed between a spike in neuron i and the receipt of the next input by neuron i, whereas recovery intervals (tr_i) denote the time elapsed between the receipt of an input by neuron i and the next spike in neuron i. The time intervals are variable and indexed by cycle number n.

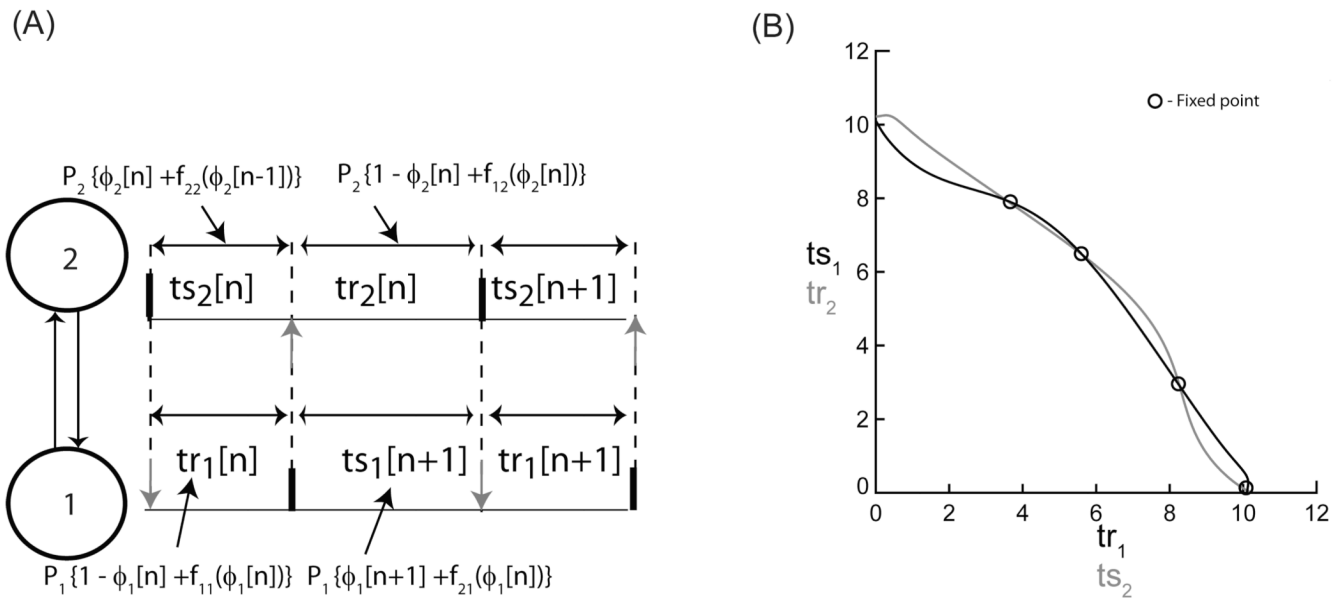

FIGURE 5.

Existence and stability analysis for two bidirectionally pulse coupled oscillators. (A) Firing map for 1:1 phase locking. The two oscillators are labeled as 1 and 2, respectively. Stimulus intervals in a phase locked mode are shown here. The black vertical bars indicate firing times and the gray vertical arrows indicate neuronal inputs at phase ϕ_i (= ts / P_j). $P_{,i}$, f_{1i} and f_{2i} represent the intrinsic period, the first order resetting and the second order resetting of the i^{th} oscillator, respectively. (B) Graphical method for determining the fixed points for the firing map given in (A). The intersections of the two curves (black and gray) indicate intervals at which the two periodicity criteria $tr_1=g(ts_1)$ and $ts_2=g^{-1}(tr_2)$ are satisfied. The circle and the cross symbols indicate the stable and unstable fixed points of the discrete map given in (A).

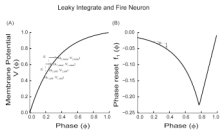

FIGURE 6.

PRC for a leaky integrate and fire neuron with a monotonically increasing evolution function ($V(\phi)$). (A) Plot of membrane potential ($V(\phi)$) versus the phase (ϕ) with $V'(\phi) > 0$ and $V''(\phi) < 0$. Since $V(\phi)$ is monotonic, the order $\phi_{1,old} < \phi_{2,old}$ is preserved after a ε perturbation ($\varepsilon > 0$) so that $\phi_{1,new} < \phi_{2,new}$. (B) The PRC as given by (24). As a result of the perturbation in (A), the old phases are advanced to new phases resulting in new phase resettings as indicated. Note that the slope of the PRC i.e. $f'_1(\phi)$ is 1 for ϕ near 1 since the PRC in these cases is constrained by causality.

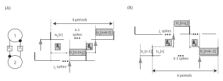

FIGURE 7.

Neural firing time map with delays of arbitrary lengths for a circuit of two pulse coupled neurons. Only two out of the four possible firing patterns are shown. The delay between a spike in neuron 1 (2) and the receipt of an input by neuron 2 (1) is designated δ_1 (δ_2). The delay between a spike in neuron 1 (2) and the receipt of an input by neuron 2 (1) is designated δ_1 (δ_2). (A) The quantities highlighted in gray sum to k cycles in neuron 1. The number of spikes that occur in neuron 2 during δ_1 is j_2. (B) The quantities highlighted in gray sum to k cycles in neuron 2. The number of spikes that occur in neuron 1 during δ_2 is j_1. Stimulus intervals (ts_i) denote the time elapsed between a spike in neuron i and the receipt of the next input by neuron i, whereas recovery intervals (tr_i) denote the time elapsed between the receipt of an input by neuron i and the next spike in neuron i. The time intervals are variable and indexed by cycle number n.

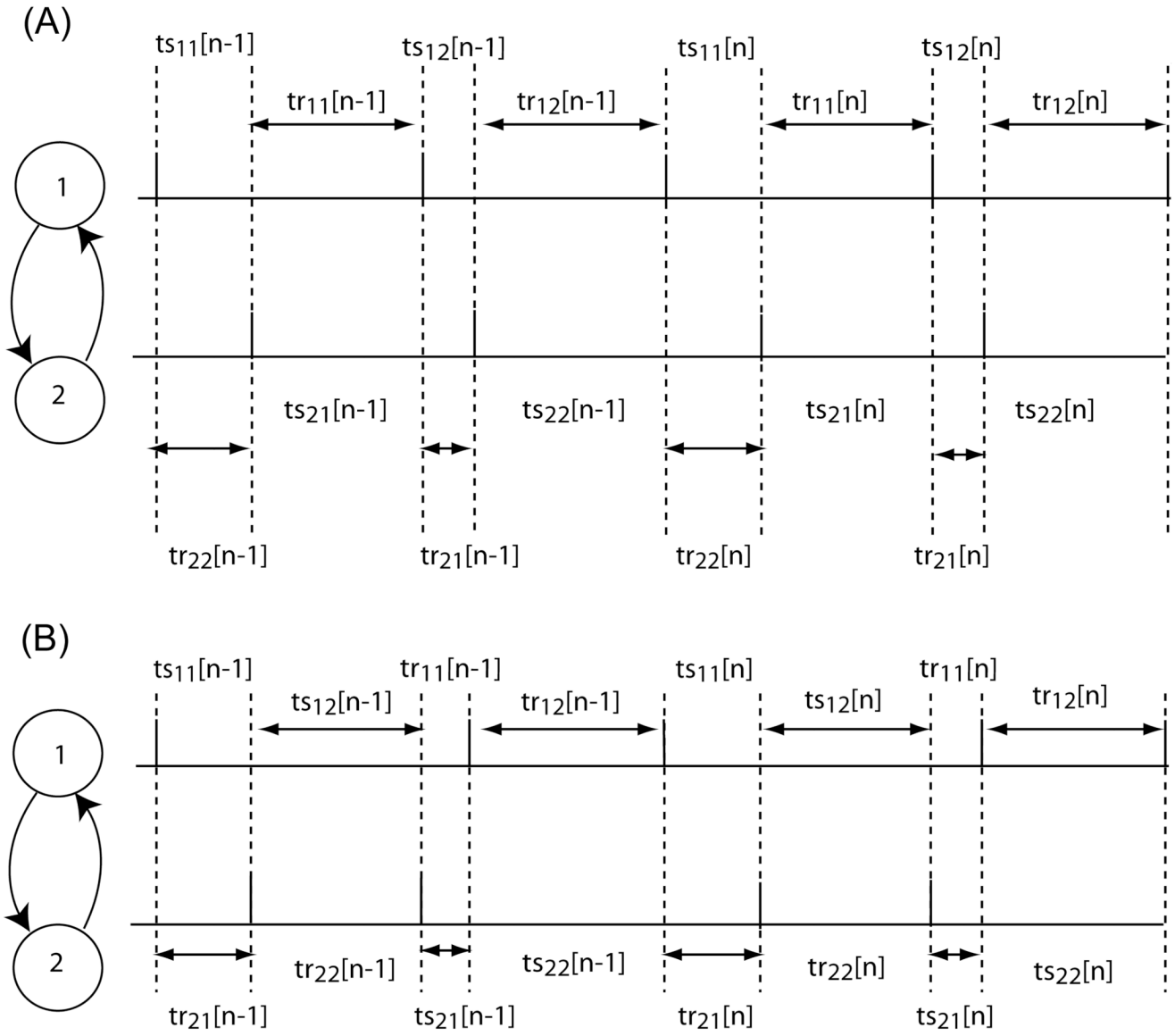

FIGURE 8.

Firing pattern for 2:2 lockings. (A) Firing order is preserved. The stimulus intervals (ts_{ij}) represent the time elapsed between the firing of neuron i and the reception of the input j from the other neuron. The recovery intervals (tr_{ij}) represent the time elapsed between the receipt of the input j by neuron i and the next spike fired by neuron i. (B) Firing order is not preserved. Note that the firing order changes on every cycle. The definitions for the ts_{ij} and tr_{ij} are different than in (A) because the assumed firing pattern is different (see [15]).

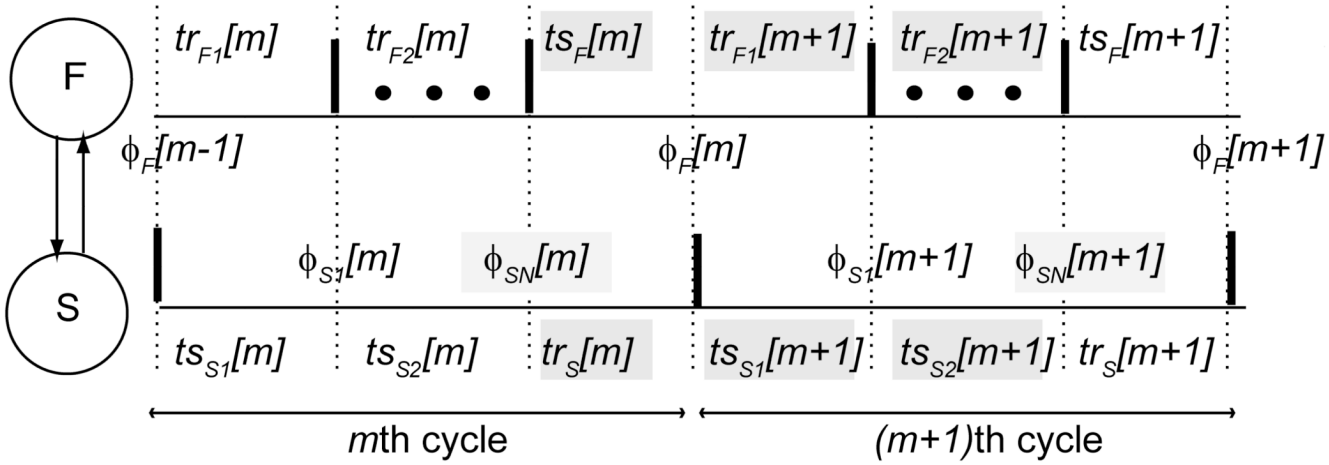

FIGURE 9.

The firing pattern for N:1 locking between two pulse coupled neurons. The faster neuron (F) fires N times for each time that the slower neuron (S) fires. Firing times are indicated by thick vertical bars. The input phases ϕ are defined on the upper and lower traces for dotted lines corresponding to a vertical bar on the partner trace indicating the time of a spike in the partner. Only the first and last spikes of the fast neuron within each cycle of the slow neuron are shown, the remaining spikes are indicated by the dots. The stimulus (ts) and recovery (tr) intervals are the time elapsed between vertical dotted lines. Both phases and intervals are subscripted by the neuron and indexed by the cycle. The second subscript on the phases of the slow neuron indicates the j^{th} input during the current cycle of the slow neuron (cycles m and m+1 are shown). The intervals highlighted in gray are defined in the text and used to construct a discrete map from $\phi_{SN}[m]$ to $\phi_{SN}[m+1]$, the phases highlighted in gray.

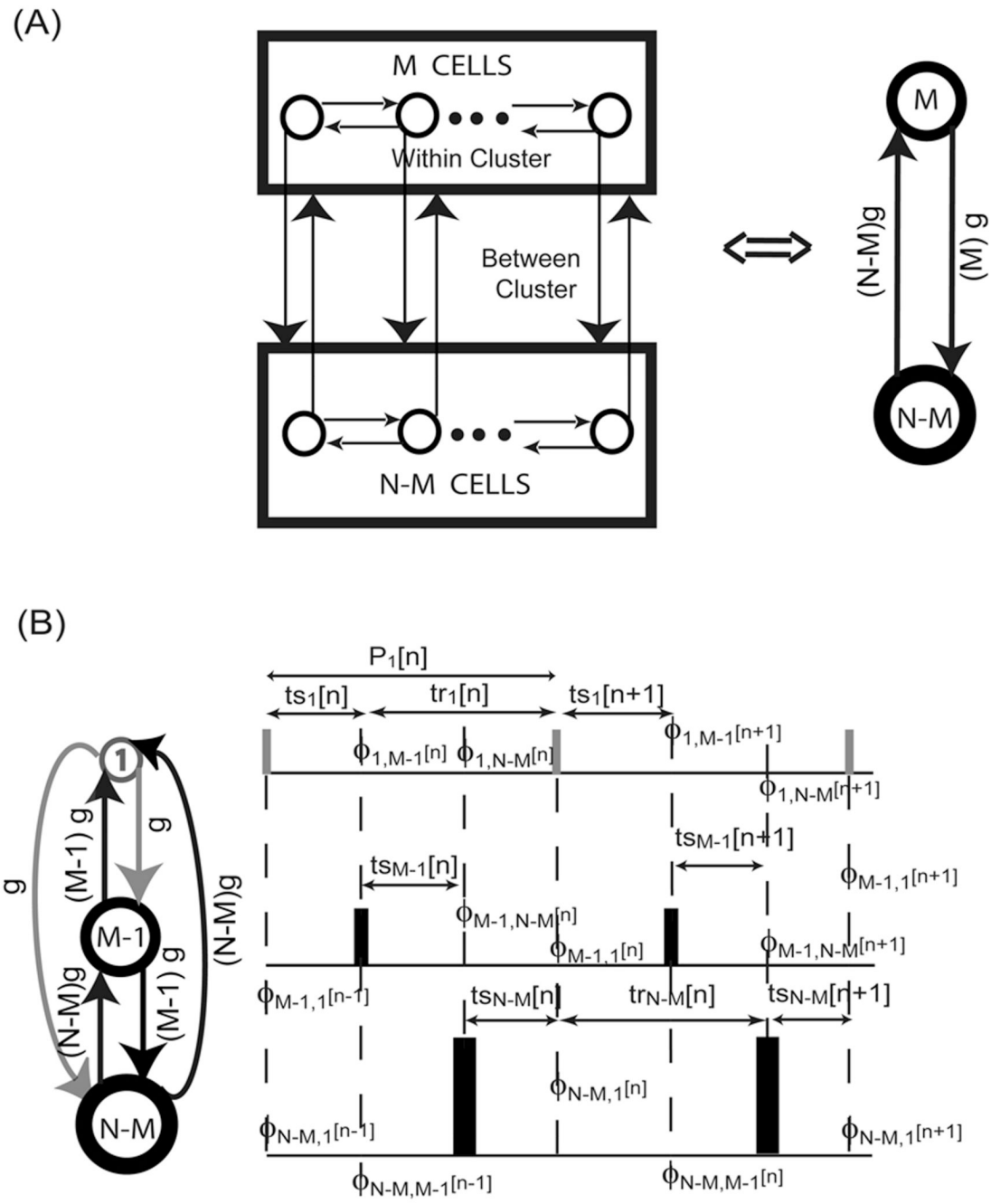

FIGURE 10.

Two populations (clusters) of M and N–M neurons, respectively. (A) Cluster interactions were analyzed by collapsing the neurons within each cluster to a single oscillator and by determining the existence and stability of a splay mode (see text section III.4.2) between two such oscillators using M times and N–M times the conductance for a single synapse, respectively. (B) A presumed perturbation map of the antiphase firing mode between M neurons in one cluster and N–M neurons in the second cluster. A perturbation of a single neuron away from the synchronous firing of M neurons was assumed. $\phi_{ij}[k]$ refers to the phase of the i^{th} neuron or cluster due to an input from the j^{th} neuron or cluster. The dashed

vertical lines in (B) indicates the firing times with an assumed sequential firing order. The strength of the synapses is indicated across the vertical arrows in (A) and (B).

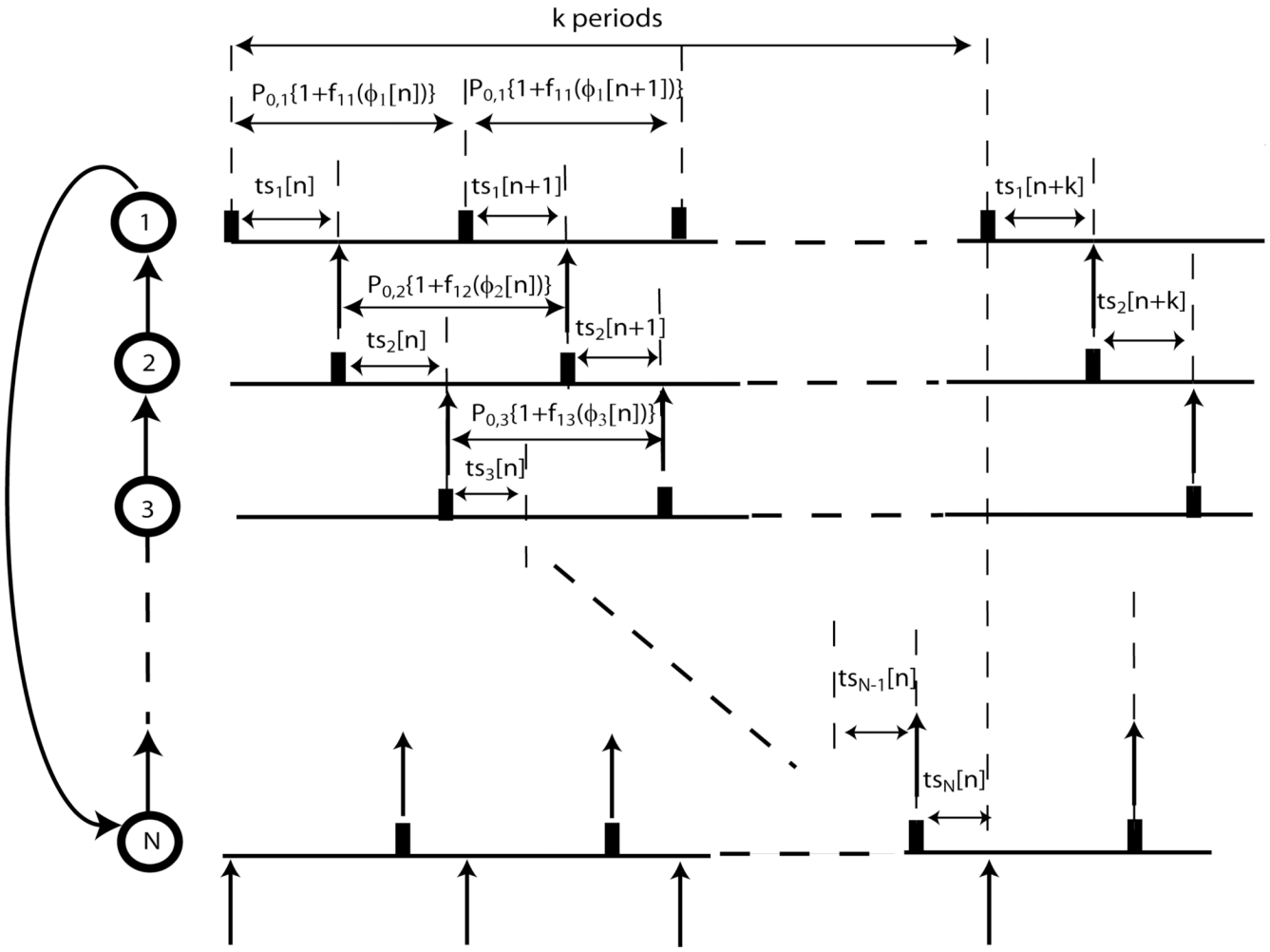

FIGURE 11.

Stability analysis for unidirectional N-ring pulse coupled oscillators. The analysis depends on k because the sum of $ts_i[n]$ for i=1 to N equals kP_e at steady state, where P_e represents the common entrained period of the N neurons. If the firing time of neuron 1 is perturbed slightly from steady state, the effects of this perturbation will propagate all the way around the ring in k periods.

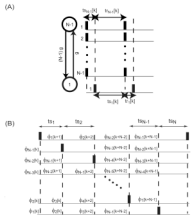

FIGURE 12.

Presumed firng patterns for synchrony and splay firing modes. (A) One cluster of N neurons. A perturbation of a single neuron away from the synchronous firing was assumed. (B) Splay firing pattern in a network of N neurons. $\phi_i[k]$ indicate the phase of the non-firing oscillators just before the k^{th} spike in the reference oscillator which produces the i^{th} input to the other (N–1) oscillators. The stimulus (ts) and response intervals (tr) in (A) and (B) can be written in terms of the phases under the assumption of pulsatile coupling, allowing the construction of discrete maps of the successive phases. The dashed vertical lines in (A) and (B) indicate the firing times with an assumed sequential firing order. The strength of the synapses is indicated across the vertical arrows in (A) and (B). The synaptic conductance strength of each neuron in (B) was assumed to correspond to that of a single neuron.